ORNL/TM-2019/1369

Comparing Wall Performance Predicted from Hygrothermal Simulations with Wall Performance Measured from Environmental Chamber Experiments

Philip Boudreaux
Mikael Salonvaara
Florian Antretter
Andre Desjarlais

December 2019

OAK RIDGE NATIONAL LABORATORY
MANAGED BY UT-BATTELLE FOR THE US DEPARTMENT OF ENERGY

ORNL/TM-2019/1369

Energy and Transportation Science Division

COMPARING WALL PERFORMANCE PREDICTED FROM HYGROTHERMAL SIMULATIONS WITH WALL PERFORMANCE MEASURED FROM ENVIRONMENTAL CHAMBER EXPERIMENTS

Philip Boudreaux
Mikael Salonvaara
Florian Antretter
Andre Desjarlais

December 2019

Prepared by
OAK RIDGE NATIONAL LABORATORY
Oak Ridge, TN 37831-6283
managed by
UT-BATTELLE, LLC
for the
US DEPARTMENT OF ENERGY
under contract DE-AC05-00OR22725

CONTENTS

LIST OF FIGURES

LIST OF TABLES

ABSTRACT

To effectively mitigate established perceptions of potential moisture risks in high-R wall assemblies (walls >R-30), a comprehensive moisture durability assessment that incorporates Building America team field evaluations, laboratory tests, and simulations has been completed over the past few years. In FY 2018, three stick-built walls were succumbed to typical Chicago, Illinois weather conditions in Oak Ridge National Laboratory's Heat, Air and Moisture chamber. The measured temperature, relative humidity, and moisture content within these walls were compared with WUFI hygrothermal simulation results. In FY 2019, similar experiments and comparisons with WUFI results were completed with two walls, a structural insulated panel-based wall and a concrete masonry unit-based wall. The following tasks were completed for these two walls:

1. **Measure air permeance** of each individual wall using ASTM E283 Standard Test Method.

2. **Test walls in diffusion scenario** as the only moisture transport mechanism, and compare measured transient temperature and relative humidity of select wall components with Chicago summer and winter weather conditions with WUFI model results.

3. **Test walls in wetting event scenario** and compare measured transient temperature and relative humidity of select wall components with Chicago summer weather conditions with WUFI model results.

4. **Test walls in diffusion/advection scenario.** In addition to controlling the outdoor chamber to match real outdoor weather conditions, a pressure differential across the wall was varied. Measured transient temperature and relative humidity of select wall components were compared with WUFI model results.

5. **Test walls in diffusion/advection with solar heating of cladding.** In addition to the variables above, heat lamps were used to heat the cladding on a diurnal cycle. Measured transient oriented strand board moisture content and temperature were compared with WUFI model results.

This report documents the experimental method, results, and comparison of the measured experimental hygrothermal performance of the two walls to simulation results, showing that hygrothermal simulations can be successfully used to predict the performance of these wall systems for the moisture transport phenomenon described above.

1. INTRODUCTION

Buildings accounted for 41% of the primary energy consumption (40.2 quads of energy) in the United States in 2010 (DOE 2014). Of this energy, 15.1 quads were consumed by the space heating and cooling of commercial and residential buildings (DOE 2014). Of this amount, 5.8 quads are attributable to roofs and walls and 4 quads to infiltration. Based on these data, reducing thermal conduction and increasing envelope air-tightness are key factors in reducing the energy consumption in buildings. Applicable research has been completed and updated building energy codes have increased the required air tightness and thermal resistance in new constructions across the United States, thereby decreasing the energy consumption of new residential homes by over 30% since 2006. This trend is shown in Figure 1. According to simulation studies by the National Association of Home Builders, the 2009 and 2012 IECC codes decrease the site energy consumption of the 2006 code-built home by 10.7% and 33.7%, respectively ("2009 IECC Cost Effective Analysis" 2012; "2012 IECC Cost Effective Analysis" 2012).

According to Pacific Northwest National Laboratory, the 2015 IECC code decreases the site energy consumption of a 2015 code-built home by 1% more than the 2012 code (Mendon et al. 2015).

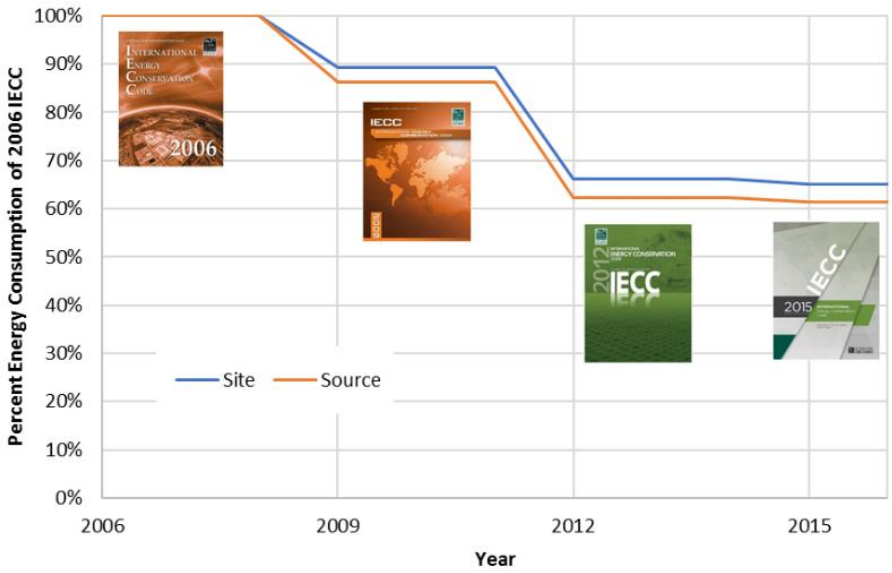

Figure 1. International building codes have decreased the energy consumption of new residential buildings by over 30% since 2006.

As building envelopes have become more energy-efficient, another challenge has arisen. Moisture plays a key role in building performance. Unwanted moisture can cause mildew, mold, wood rot, fastener corrosion, material degradation through freeze-thaw cycles, condensation on cold surfaces within the envelope, and more. Studies have shown that highly insulated walls have a great risk of high moisture, which can cause structural and health problems. According to Building America, high-R wall assemblies (walls >R-30) have many hours throughout the year when condensation can potentially form inside the wall ("High-R Walls" 2013).

Oak Ridge National Laboratory is developing a web tool, built on a rule-based expert system, that aids stakeholders in designing energy-efficient moisture-durable walls. Currently, the tool's expert system database is mostly populated with expert opinion, but work is being done to incorporate durability assessment based on stochastic hygrothermal modeling. To validate the hygrothermal models that are being used, chamber experiments have been conducted to compare measured temperature and humidity with those the hygrothermal model predicts when the boundary conditions are matched in the model to the experiment. The results from four experiments compared with hygrothermal modeling results will be presented.

2. METHODS

2.1 HEAT, AIR, AND MOISTURE CHAMBER

To complete the experimental test, the Heat, Air, and Moisture Penetration (HAM) chamber at Oak Ridge National Laboratory (ORNL), shown in Figure 2, was used. This moisture penetration test chamber can simulate interior and exterior environments on either side of the wall. The HAM chamber specifications are shown in Table 1.

Table 1. HAM chamber specifications.

	Indoor chamber	Outdoor chamber
Dry bulb temperature (°F)*	30–90	0–110 (ramp rate 1–1.5°/min)
RH [%]*	10–90	10–90
Dew point (°F)*	7–80	−5–90
Pressure (w.r.t ambient) (Pa)*	0–75 (sustained)	±1200 (pulsed) ±75 (sustained)
Precipitation	—	≤1 ft^3/min
Precipitation temperature (°F)	—	40–95
Solar insolation*	—	≤100 W/ft^2

*Steady state and transient—diurnal cycles

Figure 2. ORNL HAM chamber. The indoor chamber slides so that the test wall can be rolled in and out.

The HAM chamber is controlled with custom LabVIEW virtual instruments, which allow the simulation of a diurnal cycle of temperature, relative humidity (RH), differential pressure, and solar insulation in the chamber. The sensors used for feedback control of the interior and exterior chamber air are listed in

Table 2. Table 3 shows other sensors used to measure the temperature, RH, and moisture content inside the test wall and the volumetric airflow through the wall.

Table 2. Sensors used in feedback control loop of climate chamber environment.

Sensor	Model	Range	Accuracy
Temperature (°F)	Vaisala HMT330	−40–176	±0.36 @ 68
RH (%)	Vaisala HUMICAP 180	0–97%	±0.6% RH (0 to 40% RH) @ 68°F ±1% RH (40 to 97% RH) @ 68°F
Pressure (lb/ft^2)	Rosemount 2051CD	±288,000	±0.075% FS

Table 3. Sensors used to measure the hygrothermal state of the test wall materials and the airflow through the wall.

Sensor	Model	Range	Accuracy
Temperature (°F)	Type T Thermocouple	−380–392	±1.8
RH (%)	Honeywell HIH-4000-003	0–100	±3.5% RH
Flowmeter	EPI 8732 MPNH-SSS-133-DC24	0.16–32 SCFM	±(1% RDG + [0.5% FS +0.02% FS/°C])
Moisture content (%)	Temperature and species-corrected moisture pins	6–30	—

During some of the experiments, moisture content measurements were taken of the OSB in one of the walls. For these measurements, a handheld Delmhorst BD 2100 moisture meter was used. Upon the manufacturer's suggestion, the species correction table for basswood was used as a surrogate for the OSB.

2.2 EXPERIMENTAL PLAN

Two walls were tested in the HAM chamber: one based on concrete masonry units (CMUs) and the other based on structural insulated panels (SIPs). Figure 3 shows each wall assembly in detail. For the CMU-based wall, the layers—starting from the outside and moving to the interior—were 8 in. CMUs, a Sto Gold Coat, 1.5 in. of extruded polystyrene (XPS) insulation, a ¾ in. lathe strip to create an air gap between the insulation, and a ½ in. gypsum board. The SIP-based wall had layers of vinyl siding, a ¾ in. lathe strip to create air gap behind siding, Tyvek, a 4.25 in. SIP panel, and a ½ in. gypsum board. The SIP panel had 7/16 in. OSBs on either side with R-16 of expanded polystyrene (EPS) insulation between the OSBs.

Figure 4 shows the location of temperature and RH sensors in each wall at two vertical locations that are ±16 in. from the middle line, which is approximately 4 ft from the wall baseplate as shown in Figure 3. Moisture content was measured at similar positions in the western cedar lathe strip in each wall. Finally, the moisture content was also measured in an embedded piece for wood (fir) on the interior side of the CMU block and on the exterior face of the SIP panel.

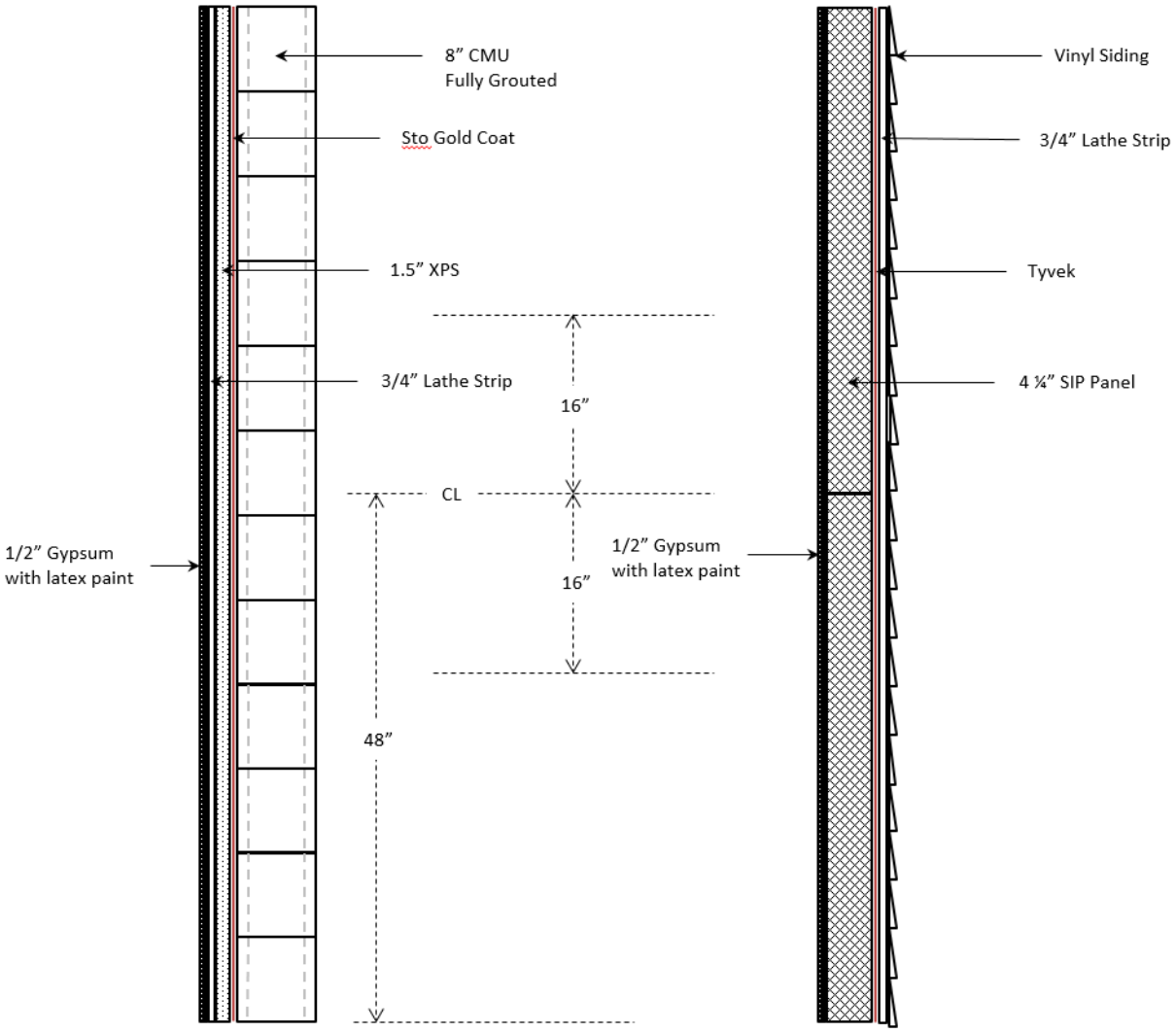

Figure 3. Assembly details of the CMU and SIP walls. The dotted lines 16 in. from the middle line show the location of the sensors in between the wall layers measuring temperature, RH, and moisture content.

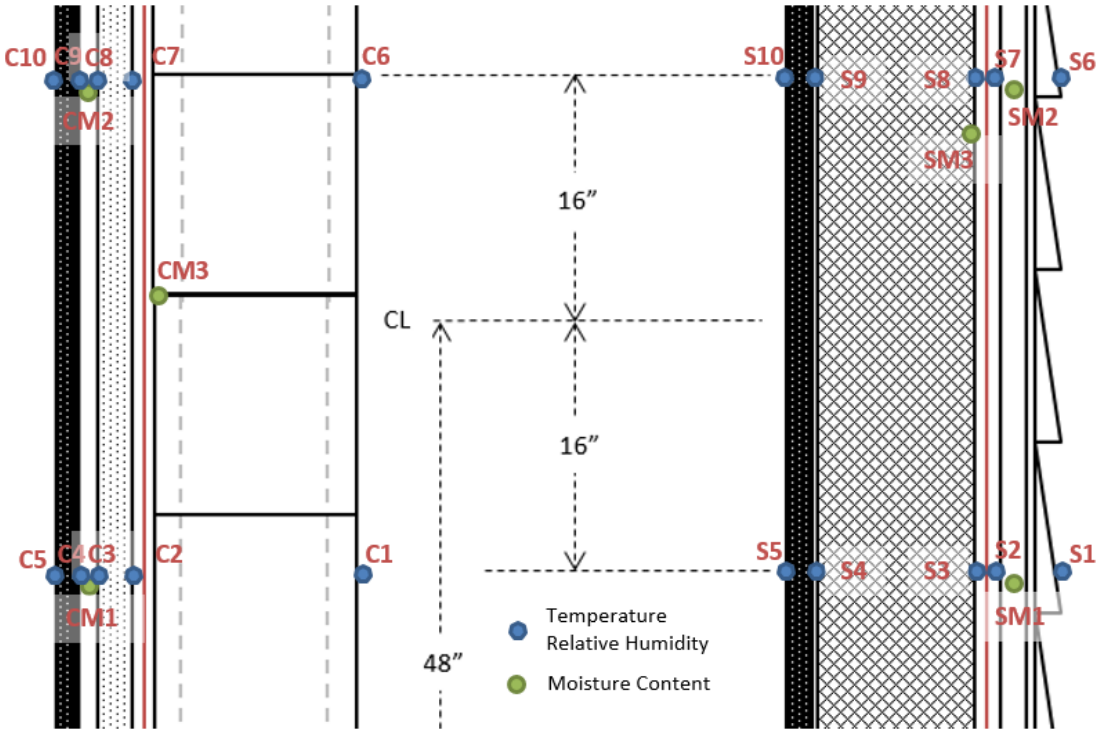

Figure 4. Location of sensors in each wall with sensor labels for the CMU wall (C) and the SIP wall (S). “SM” and “CM” represent the moisture pins in the SIP wall and CMU wall, respectively.

For the tests, both winter and summer conditions were simulated in the outdoor room of the chamber. For the interior boundary condition, the indoor chamber was set to a constant 75°F/50% RH for summer and a constant 68°F/40% RH for winter. For the exterior conditions, diurnal temperature and RH data from the Chicago, Illinois cold-year weather conditions from the WUFI database were used. When the summer conditions were simulated in the chamber, the weather conditions starting on June 1st were used, and when the winter conditions were simulated, weather conditions starting on December 15th were used. These simulated weather conditions are illustrated in Figure 5; the red box indicates the summer and the blue the winter.

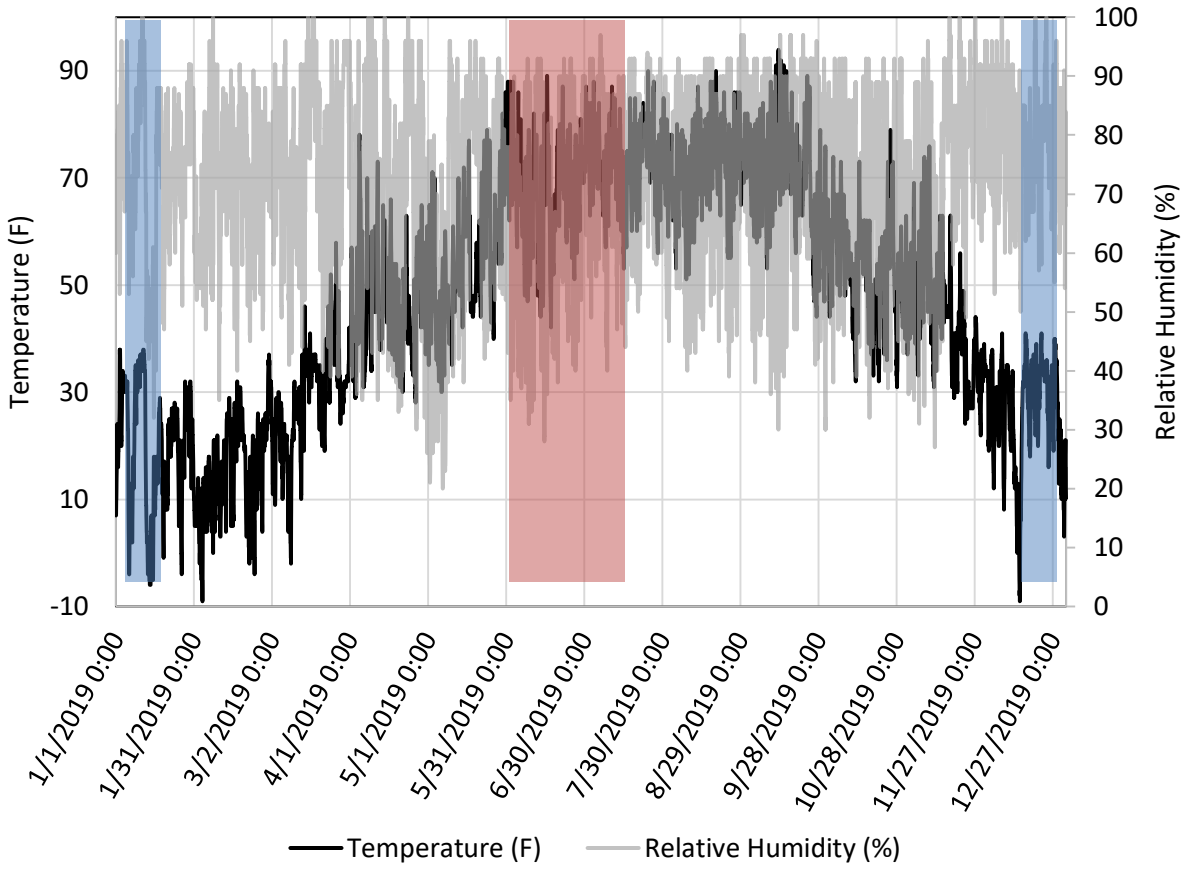

Figure 5. Exterior boundary conditions for the test wall were taken from the cold-year Chicago weather conditions file from WUFI. The red box indicates the weather conditions that were simulated in the chamber for the summer and the blue for the winter.

To effectively mitigate prevailing perceptions of potential moisture risks in high-R wall assemblies, a comprehensive moisture durability assessment incorporating laboratory tests and simulations was completed. The following tests were completed and the measured results were compared against WUFI simulation output. These tests build on each other, with each round of tests adding one new method of moisture transport.

1. **Test walls in diffusion scenario** as the only moisture transport mechanism, and compare measured transient temperature and RH of select wall components under Chicago summer and winter weather conditions with WUFI model results.

2. **Test walls in wetting event scenario** and compare measured transient temperature and RH of select wall components under Chicago summer weather conditions with WUFI model results.

3. **Test walls in diffusion/advection scenario.** In addition to controlling the outdoor chamber to match real outdoor weather conditions, the pressure differential across the wall was varied. Measured transient temperature and RH of select wall components were compared with WUFI model results.

4. **Test walls in diffusion/advection with solar heating of cladding.** In addition to the variables above, heat lamps were used to heat the cladding on a diurnal cycle. Measured transient OSB moisture content and temperature were compared with WUFI model results.

2.3 CHARACTERIZING WALL INFILTRATION

Before the tests outlined above were completed, the air infiltration of each wall was determined using the ASTM E283 Standard Test Method. To measure the volumetric airflow rate versus pressure differential, a calibrated EPI thermal mass flowmeter was used as described in Table 3. To determine the leakage of each wall, the baseline air leakage was first characterized for the whole test frame. Then, the air leakage was characterized when the SIP wall was sealed with plastic, and then again when just the CMU wall was sealed with plastic as shown in Figure 6. The difference between the baseline and one of these tests describes the leakage for a wall.

Figure 6. To determine the leakage of each wall, the walls were covered and sealed with plastic sheathing.

The leakage was characterized as the power law shown in Eq. (1), where C is the flow coefficient and n is the flow exponent, which are both found experimentally; P is the pressure differential across the wall and Q is the resulting volumetric airflow through the wall.

$$Q = C\ P^n \qquad \text{Eq. (1)}$$

Table 4 shows the results of the leakage at 75 Pa for each of the situations described above with the last three columns showing the leakage of the CMU and SIP walls. Notice that both walls are very tight, significantly less than the current Army requirement of ~1.3 L/s m^2.

Table 4. Results from leakage test of the SIP and CMU walls.

	Pressurization @ 75 Pa (CFM)	Difference between baseline and covered wall		
		(CFM)	(L/s)	(L/s m^2)
Full wall (baseline)	4.693	—	—	—
SIP covered	4.678	0.015	0.007	0.002
CMU covered	4.369	0.325	0.153	0.051

2.4 HYGROTHERMAL MODEL

WUFI Pro—the model used in this project—is a transient, one-dimensional heat and moisture transfer model that can assess the hygrothermal behavior of a construction. WUFI is a commonly used building industry hygrothermal model and is one of the most advanced hygrothermal models for coupled mass and heat transport analysis (IBP 2012). WUFI is based on a state-of-the-art understanding of physics regarding sorption and suction isotherms, vapor diffusion, liquid transport, and phase changes. The model is also well documented and has been validated by many comparisons between calculated and field performance data (Holm and Kunzel 1999; Kunzel 1995; Kunzel, Kiebl, and Krus 1995; Kunzel and Kiebl 1996).

The necessary input data include the composition of the component, its orientation and inclination, the initial conditions, and the time period of interest. The material parameters and climatic conditions can be selected from the embedded databases, or the actual data can be input if their hygrothermal properties have been measured. A materials database that is part of the program includes a full range of building and insulation materials commonly used in the building industry, and user-defined materials can easily be added to the database as needed. The model requires hourly weather conditions data such as temperature, RH, wind speed and orientation, driving rain, and solar radiation, which are employed in the hygrothermal calculations. These data are available in a database for a wide range of global climatic zones, and specific climate data can be added if needed.

The model accounts for solar radiation and night sky radiation since these can be important thermal and moisture loads in various climates around the world. The night sky radiation feature allows one to consider surface wetting during the night. The model also contains algorithms for modeling the effect of wind-driven rain as a function of height. Interior conditions are set or can vary depending on the time of year and day, and they can be determined by various built-in models to account for indoor thermal and moisture loads.

WUFI Pro is an excellent tool for understanding the complex interactions during the transport of heat and moisture in construction assemblies. The visual design allows one to understand the complex effects that nonlinear material properties play in the transport of moisture. Post-processing can be done in the tool, for example, to estimate the risk of mold growth by using the ASHRAE Standard 160-approved Mold Growth Index model developed by Viitanen et al. (ASHRAE 2016; Viitanen et al. 2015).

2.4.1 Material Properties in Simulations

The materials for the simulations were taken from the WUFI databases and supplemented with some corrections as shown in Table 5. The corrected material properties are listed in Appendix A; all other materials are referred to in the WUFI material database.

Table 5. Materials used in hygrothermal simulations and the selected material properties.

Layer name	WUFI database material
CMU exterior wall	Listed in Appendix A
Concrete fill	Concrete screed, mid-layer
Fluid-applied vapor-permeable air/moisture barrier	GE Elemax 2600 AWB
XPS, 1.5 in.	Listed in Appendix A
Furred air cavity, ¾ in.	Air layer 20 mm; without additional moisture capacity
Interior gypsum board, ½ in.	Gypsum board (USA)
OSB, 7/16 in.	Listed in Appendix A
Weather-resistive barrier	Spunbonded polyolefin
EPS insulation	EPS insulation

3. DISCUSSION OF RESULTS

3.1 DIFFUSION TESTS

This test investigated the effects of water vapor movement by diffusion on the RH inside a wall. The measured transient in situ RH in key locations were compared with WUFI modeling results. In the experiments, the indoor chamber was kept at a static temperature and RH, and the outdoor chamber followed a typical Chicago weather diurnal cycle. The Chicago weather simulation accuracy is presented and the experimental and modeled RH inside the wall are compared.

3.1.1 Summer

For the summer diffusion test, 26 days of Chicago weather conditions were simulated beginning on June 1st of the Chicago cold-year weather conditions file from WUFI. Figure 7 shows how well the exterior chamber environment was controlled to capture the weather conditions described in the file. For all but 4 h of the 26-day experiment, the chamber temperature and RH were within 10% of the target temperature and RH.

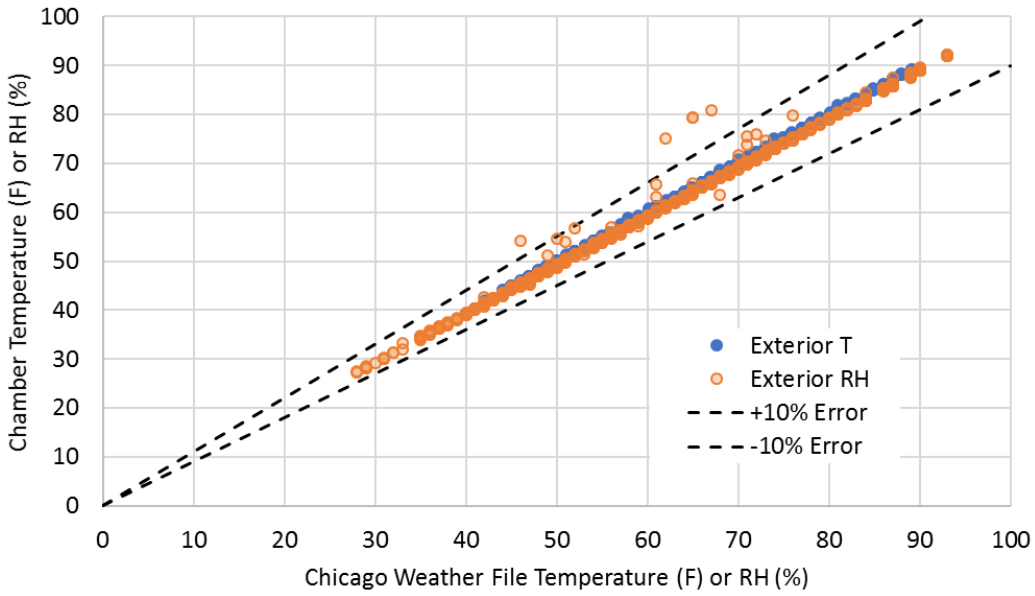

Figure 7. The chamber environment was controlled within 10% of the target temperature and RH during the 26-day summer diffusion test.

3.1.1.1 Simulated and monitored performance of the CMU wall—Chicago summer

Simulations were started one week before measured data collection to precondition the wall to the initial condition of 35% RH. Figure 8 shows the layer layout for the CMU wall as it was modeled in WUFI. The layers from outside to inside are

1. CMU exterior wall
2. Concrete fill
3. CMU interior wall
4. Fluid-applied vapor-permeable air/moisture barrier (Sto Gold Coat TA)
5. XPS, 1.5 in.
6. Furred air cavity, ¾ in.
7. Interior gypsum board, ½ in.

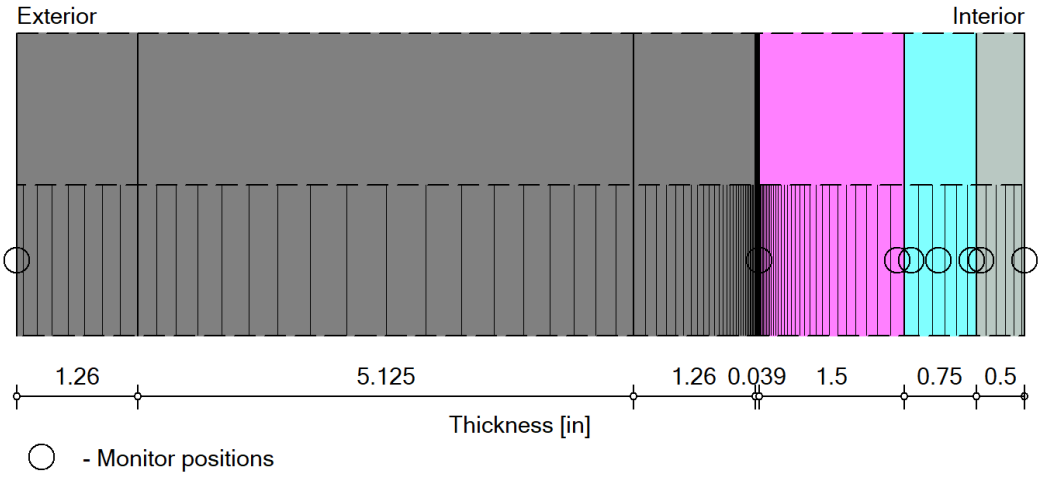

Figure 8. CMU wall assembly as modeled in WUFI.

Figure 9 shows the measured temperature and RH at two locations on the interior side of the XPS insulation in the CMU wall for the duration of the chamber test compared with the hygrothermal simulation results. The simulation results show close agreement to the measured performance; the maximum difference is within 1.1% for temperature and 10.0% for RH when compared with the average of the two sensors in the measurements.

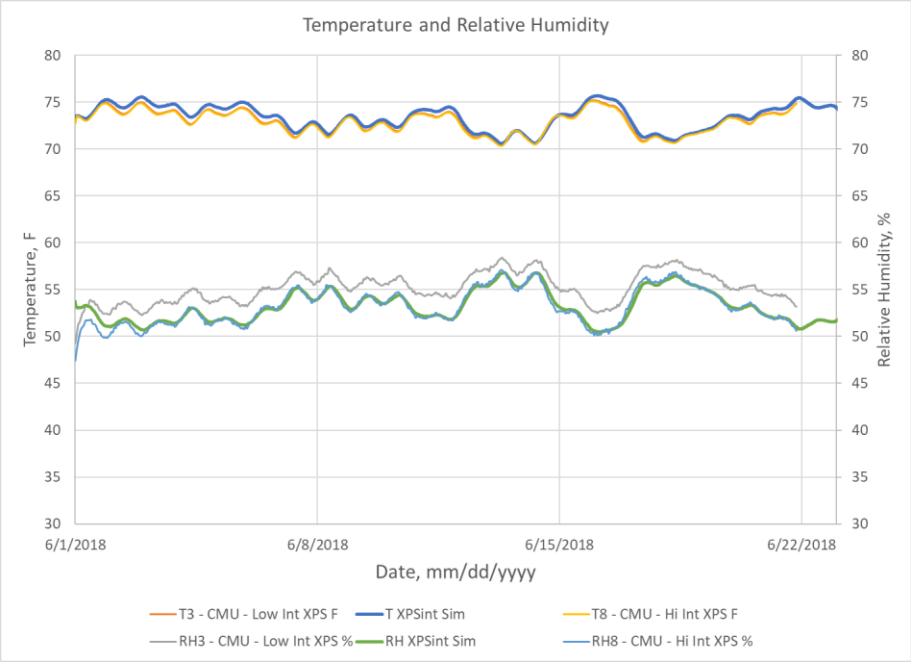

Figure 9. Simulated temperature (T XPSint Sim) and RH (RH XPSint Sim) on the indoor side surface of the XPS insulation in the CMU wall. Measured data: Sensors 3 (lower) and 8 (upper) are on the indoor side surface of the XPS. Summer conditions with only diffusion.

Figure 10 shows the measured performance of the temperature and RH at two locations on the exterior side of the XPS on the CMU wall compared with simulation results. The simulation results show close agreement to the measured performance; the maximum difference is within 3.9% for temperature and 11.2% for RH when compared with the average of the two sensors in the measurements.

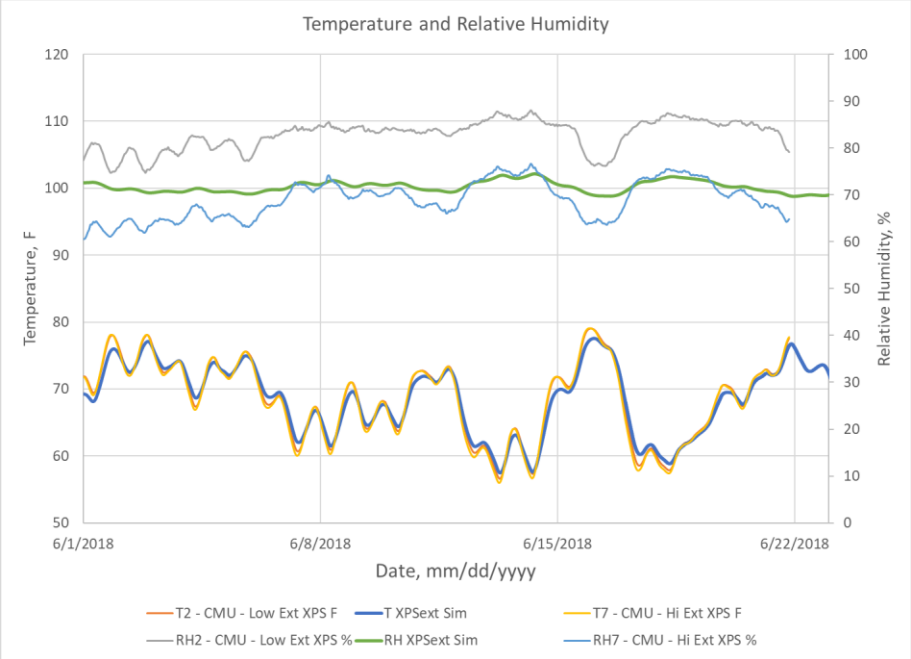

Figure 10. Simulated temperature (T XPSext Sim) and RH (RH XPSext Sim) on the exterior side surface of the XPS insulation in the CMU wall. Measured data: Sensors 2 (lower) and 7 (upper) are on the exterior side of the XPS. Summer conditions with only diffusion.

3.1.1.2 Simulated and monitored performance of the SIP wall – Chicago Summer

For the summer diffusion test, the simulation was set to an initial condition of 60% RH in the SIP wall. Figure 11 shows the layer layout for the SIP wall as it was modeled in WUFI. The layers from outside to inside are

1. Vinyl siding
2. Furred air cavity, ¾ in.
3. Water resistive barrier (WRB; spunbonded polyolefin)
4. Air gap, 0.039 in. (mechanically fastened membrane, space for a sensor reading)
5. SIP panel
    a. OSB, 7/16 in.
    b. EPS, 3.6 in.
    c. OSB, 7/16 in.
6. Interior gypsum board, ½ in.

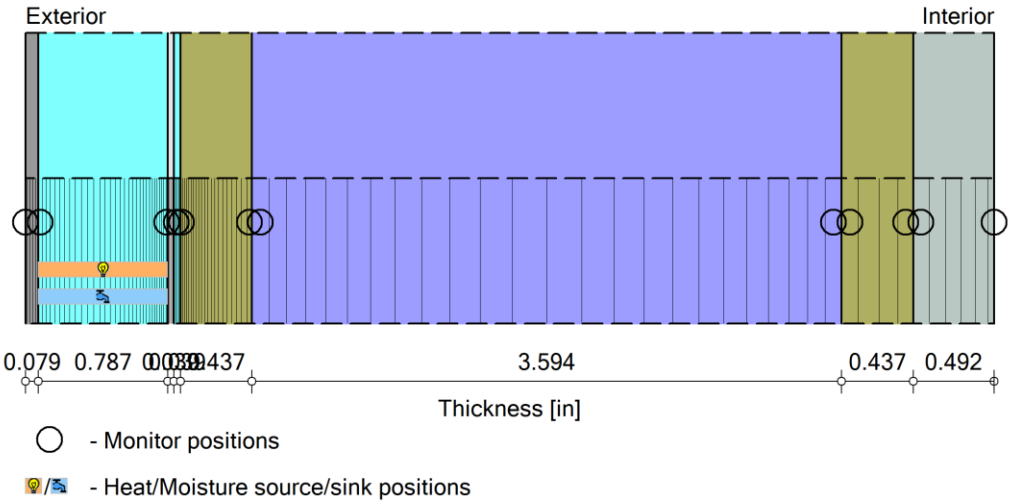

Figure 11. SIP wall assembly as modeled in WUFI.

For the simulation, the air cavity behind the vinyl siding is vented at an air exchange rate of 40 air change per hour (ACH). Lstiburek et al. suggest 200 ACH for vinyl siding, but a lower ventilation rate was chosen because of the assembly being exposed to laboratory conditions with no solar radiation or wind effects (Lstiburek, Ueno, and Musunuru 2016).

Figure 12 shows the simulated temperature and RH results from WUFI on the exterior side of the Tyvek WRB compared with the measured data. The simulated results stayed within 9.7% and 25.6% of the measured temperature and RH, respectively. Figure 13 shows the simulated temperature and RH results from WUFI on the exterior side of the SIP panel compared with the measured data. The simulated results stayed within 8.2% and 24.4% of the measured temperature and RH, respectively. Figure 14 compares the measured temperature and RH with the simulated temperature and RH on the interior surface of the SIP panel. The simulated results stayed within 3.3% and 2.4% of the measured temperature and RH, respectively.

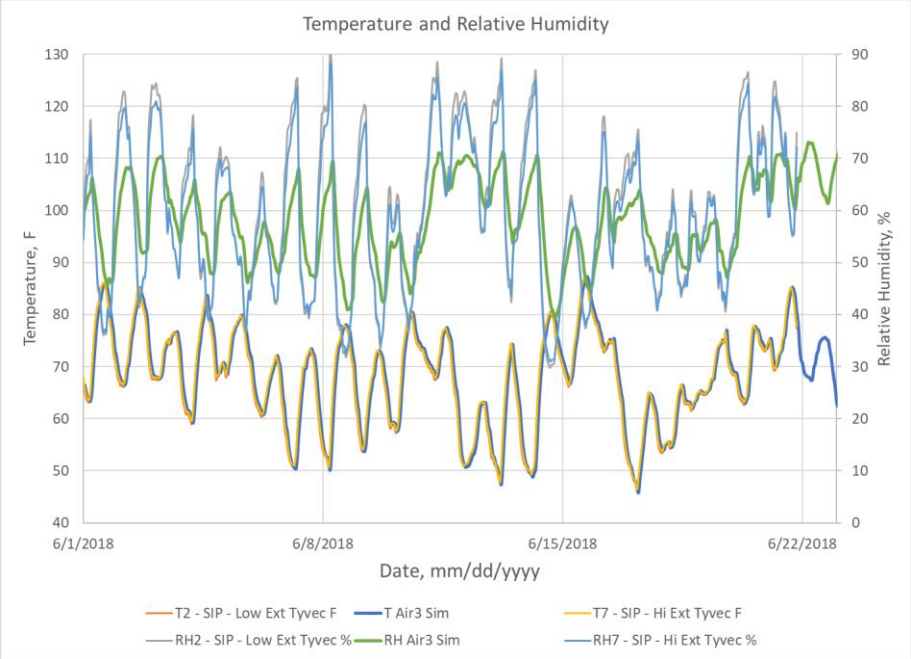

Figure 12. Simulated temperature (T Air3 Sim) and RH (RH Air3 Sim) on the exterior side of the WRB. Measured data: Sensors 2 (lower) and 7 (upper) are also on the exterior side of the WRB. Summer conditions with only diffusion.

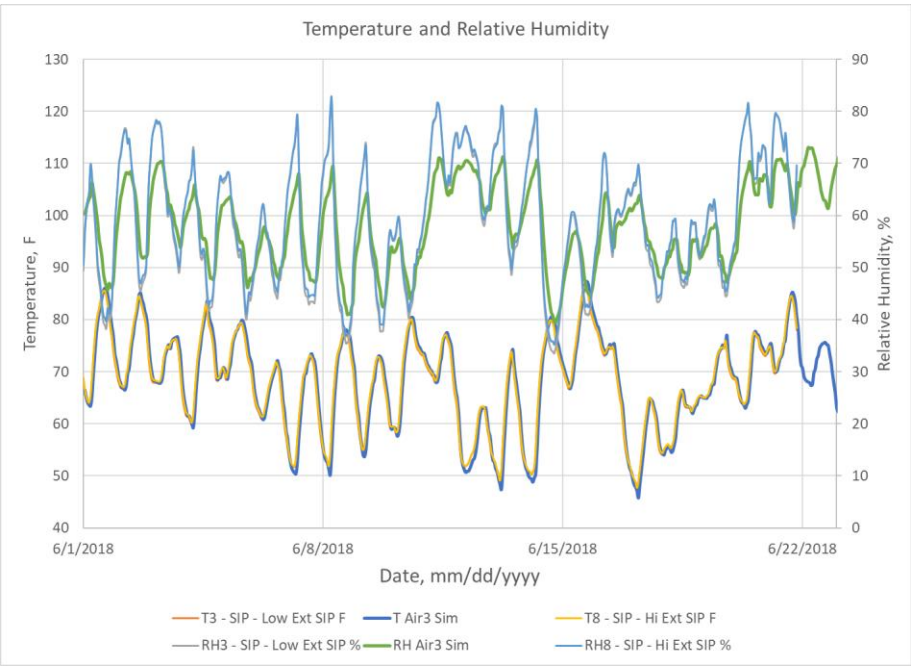

Figure 13. Simulated temperature (T Air3 Sim) and RH (RH Air3 Sim) on the exterior surface of the SIP panel between the OSB and WRB. Measured data: Sensors 3 (lower) and 8 (upper) are between the exterior OSB and WRB. Summer conditions with only diffusion.

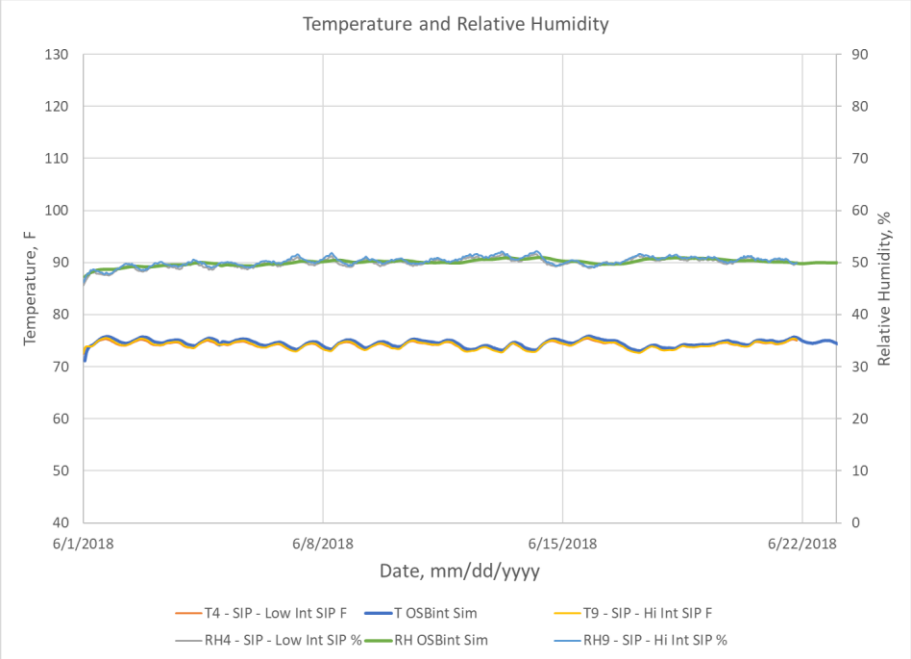

Figure 14. Simulated temperature (T OSBint Sim) and RH (RH OSBint Sim) on the interior side surface of the SIP panel between the OSB and gypsum board. Measured data: Sensors 4 (lower) and 9 (upper) are between the interior OSB and gypsum board. Summer conditions with only diffusion.

3.1.2 Winter

For the winter diffusion test, 43 days of Chicago weather conditions were simulated beginning on December 15th of the Chicago cold-year weather conditions file from WUFI. Figure 15 shows how well the exterior chamber environment matched the weather conditions described in the file. For a significant portion of the 43-day experiment, the chamber RH was well over 10% of the target, which was caused by the chamber having difficulty controlling the RH when the chamber dry bulb temperature was below freezing.

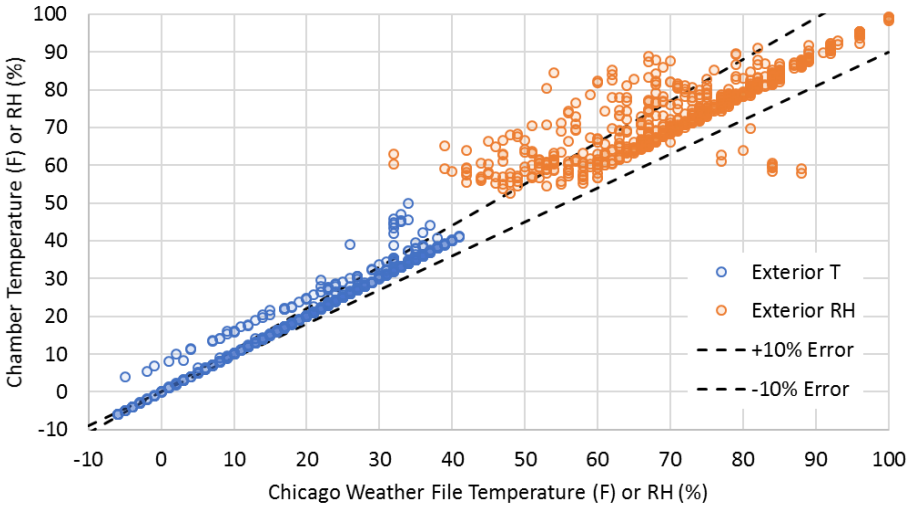

Figure 15. The chamber environment has some periods when its temperature and RH had over 10% error compared with target, especially for the RH. This result is caused by the chamber having difficulty controlling the RH at dry bulb temperatures below freezing.

3.1.2.1 Simulated and monitored performance of the CMU wall—Chicago winter

Simulations started six days before measured data collection to precondition the wall. Figure 16 shows the simulated temperature and RH results from WUFI on the exterior side surface of the XPS compared with the measured data. The simulated results stayed within 8.1% of both the measured temperature and RH. Figure 17 shows the simulated temperature and RH results from WUFI on the interior side surface of the XPS compared with the measured data. The simulated results stayed within 2.2% and 1.8% of the measured temperature and RH, respectively.

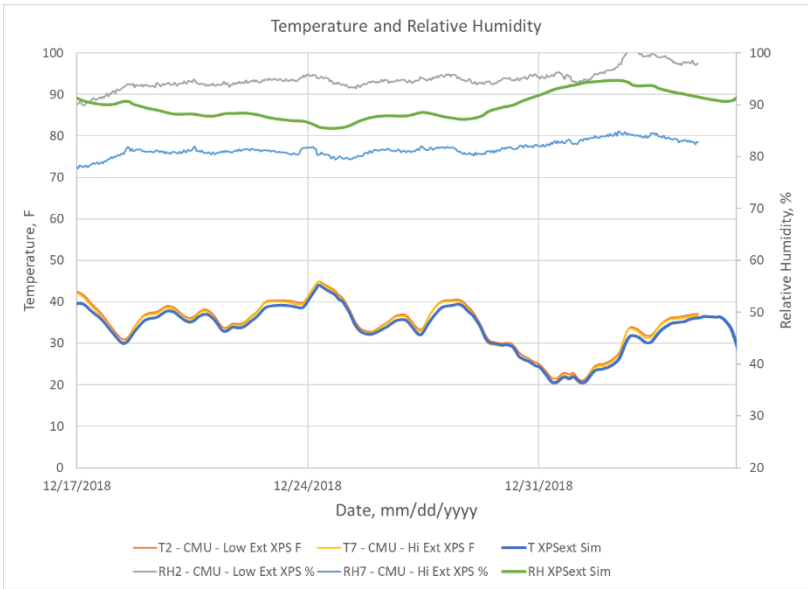

Figure 16. Simulated temperature (T XPSext Sim) and RH (RH XPSext Sim) on the exterior side surface of the XPS insulation in the CMU wall. Measured data: Sensors 2 (lower) and 7 (upper) are on the exterior side of the XPS. Winter conditions with only diffusion.

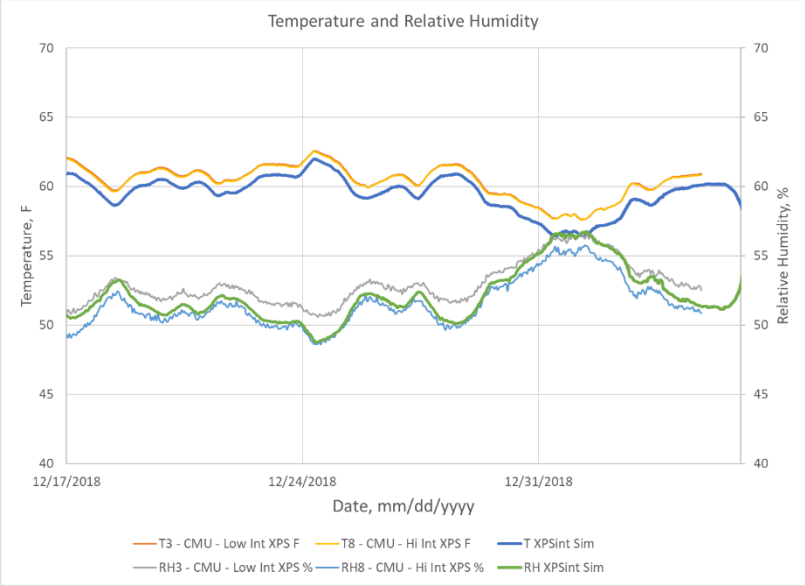

Figure 17. Simulated temperature (T XPSext Sim) and RH (RH XPSext Sim) on the interior side surface of the XPS insulation in the CMU wall. Measured data: Sensors 3 (lower) and 8 (upper) are on the interior side of the XPS. Winter conditions with only diffusion.

3.1.2.2 Simulated and monitored performance of the SIP wall—Chicago winter

Figure 18 shows the simulated temperature and RH results from WUFI on the exterior side surface of the SIP in the air gap between the WRB and siding compared with the measured data. The simulated results stayed within 17.8% and 15.7% of the measured temperature and RH, respectively.

Figure 19 shows the simulated temperature and RH results from WUFI on the exterior side surface of the SIP panel between the OSB and WRB compared with the measured data. The simulated results stayed within 16.7% and 11.9% of the measured temperature and RH, respectively.

Figure 20 shows the simulated temperature and RH results from WUFI on the interior side surface of the SIP panel between the OSB and gypsum board compared with the measured data. The simulated results stayed within 4.0% and 11.3% of the measured temperature and RH, respectively.

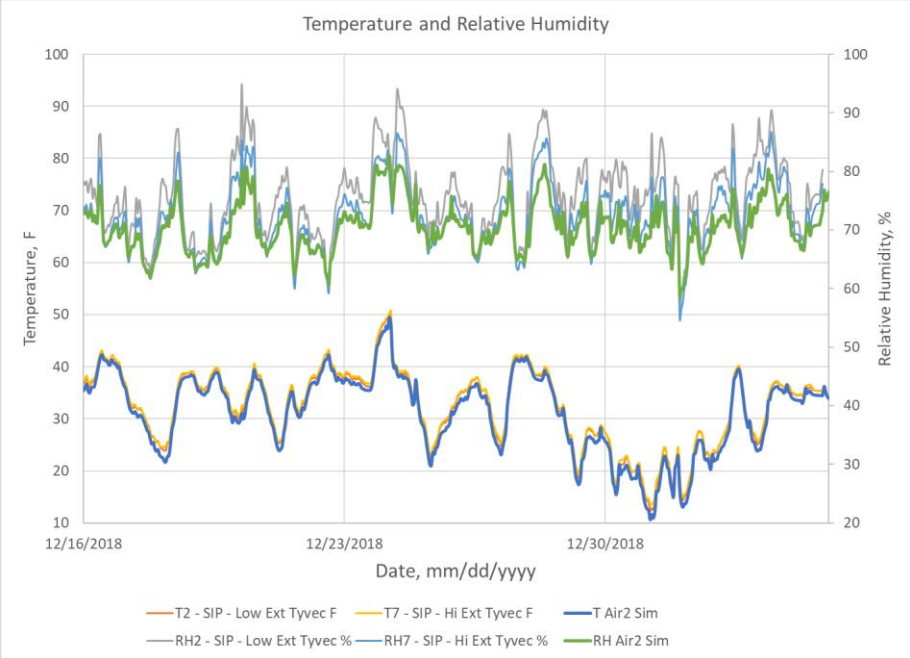

Figure 18. Simulated temperature (T Air2 Sim) and RH (RH Air2 Sim) on the exterior side surface of the SIP in the air gap between the WRB and siding. Measured data: Sensors 2 (lower) and 7 (upper) are on the exterior side of the WRB. Winter conditions with only diffusion.

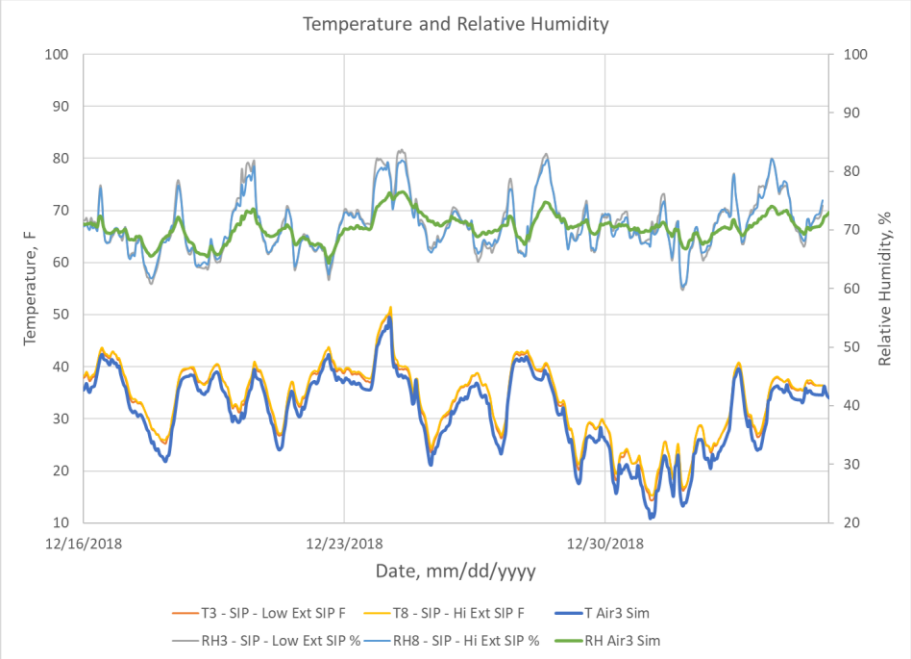

Figure 19. Simulated temperature (T Air3 Sim) and RH (RH Air3 Sim) on the exterior side surface of the SIP panel between the OSB and WRB. Measured data: Sensors 3 (lower) and 8 (upper) are between the exterior OSB and WRB. Winter conditions with only diffusion.

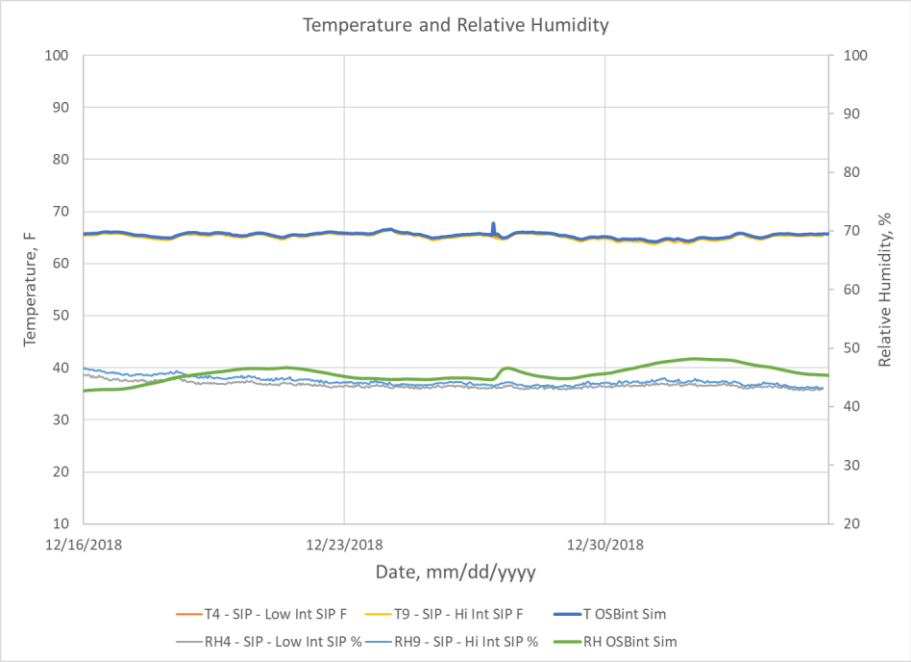

Figure 20. Simulated temperature (T OSBint Sim) and RH (RH OSBint Sim) on the interior side surface of the SIP panel between the OSB and gypsum board. Measured data: Sensors 4 (lower) and 9 (upper) are between the interior OSB and gypsum board. Winter conditions with only diffusion.

3.2 WETTING EVENT

To simulate a leak in the cladding, water-saturated 1/8 in. polypropylene sorbent sheets were placed inside the wall. To accomplish this simulation, the walls had to be partially dismantled and then reassembled. For the SIP wall, the polypropylene sorbent sheet was added between the SIP panel and Tyvek; for the CMU wall, it was added between the XPS and Sto Gold coat. In both cases, the sheet was added to the interior side of the main moisture barrier so that it would simulate damage to the weather-resistive barrier in the wall, which would let bulk water into the wall. After the dry sheet was stapled in the wall, it was misted with water. For the CMU and SIP wall, 46.99 oz and 50.7 oz of water were added, respectively. This test lasted for 21 days and was only conducted for Chicago summer weather conditions. Figure 21 shows that the temperature and RH in the chamber were controlled within 10% of the targets during the test.

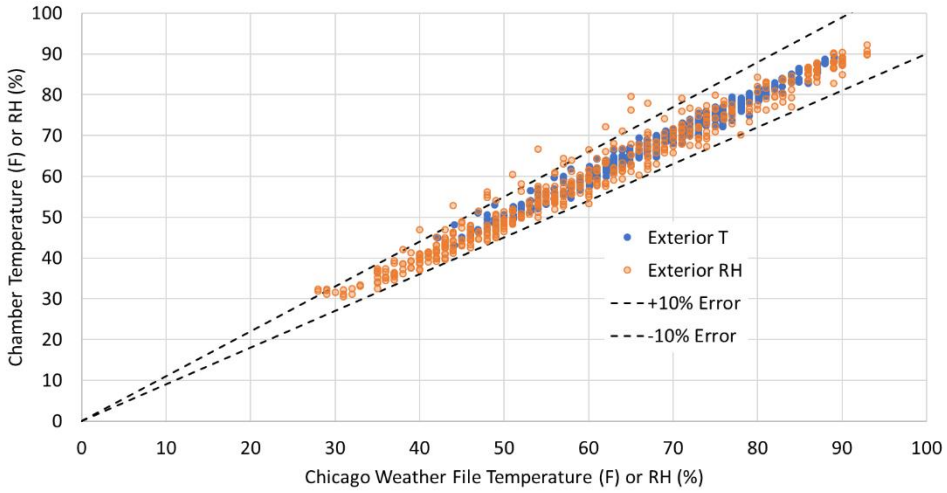

Figure 21. The chamber environment was controlled within 10% of the target temperature and RH during the most of the 21-day wetting test.

The polypropylene sorbent sheet is a fast-drying material. A simple drying test was completed in dry indoor conditions. The weight of an 18.75 in. × 8.75 in. × 1/8 in. sample at equilibrium with indoor conditions of 72.8±0.5°F and 29±1% RH was 0.055 lb [0.025 kg]. Figure 22 shows the drying of this sample over time as the gravimetric water content described in Eq. (2), where u is the gravimetric water content by percent, m_w is the mass of the water, and m_{wet} is the mass of the sample before wetting (without drying).

$$u = \frac{m_w}{m_{wet}} * 100 \qquad \text{Eq. (2)}$$

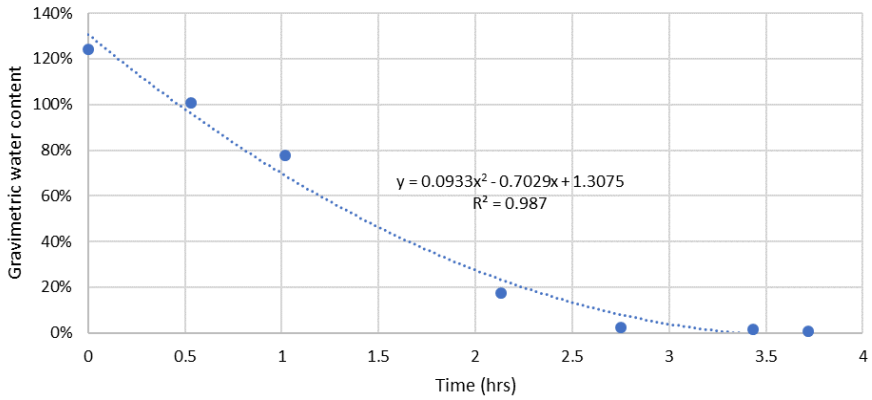

Figure 22. Gravimetric water content of a polypropylene sheet drying over time in a dry indoor environment.

The wetting event was created in the hygrothermal modeling with WUFI by setting the initial moisture content of the sorbent sheet to the tested moisture content. The amount of water added to the sorbent sheet was divided by the area and thickness of the layer in the simulation model to insert the volumetric moisture content in the sorbent material. The simulations started June 1, 2018 at 12:00 AM with the moisture in the sorbent sheet.

3.2.1 CMU Wall

Figure 23 shows the layer layout for the CMU wall as it was modeled in WUFI. The layers from outside to inside are

1. CMU exterior wall
2. Concrete fill
3. CMU interior wall
4. Fluid-applied vapor-permeable air/moisture barrier (Sto Gold Coat TA)
5. Low-density fiber glass insulation, 1/8 in., with initial moisture content to match the inserted amount of water per surface area
6. XPS, 1.5 in.
7. Furred air cavity, ¾ in.
8. Interior gypsum board, ½ in.

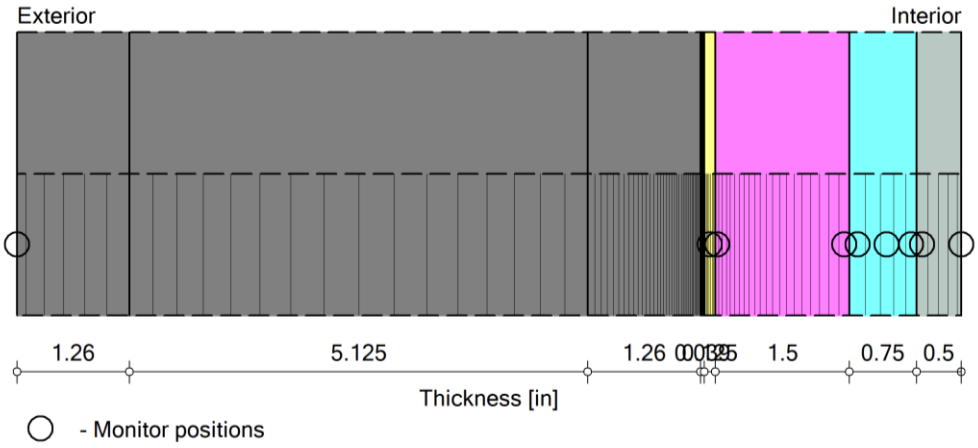

Figure 23. CMU wall assembly as modeled in WUFI with the sorbent sheet between the liquid applied air/moisture barrier and XPS.

Figure 24 shows the measured moisture content in the moisture pins in the lathe strips between the gypsum board and XPS and in the piece of wood placed between the WRB and CMU block. Figure 25 shows the simulated temperature and RH results in the absorbent layer along with the measured data. The results show that the water in the absorbent layer does not stay evenly distributed and the sensor located higher in the wall shows a lower RH than the sensor that is lower in the wall. After spraying the water in the absorbent sheet, some of the water drained out (this amount was accounted for in the amount that stayed in the wall). Gravity likely slowly pulled the water downward. The simulated results with the full water source showed that the wall dried very slowly. The results stayed within 10.5% and 26.8% of the measured (average of the high and low sensors) temperature and RH, respectively. Another simulation was carried out with half the water as a source in the absorbent sheet and these results agreed better with the drying time and the level of humidity. The simulated results with half the water source stayed within 10.6% and 12.9% of the measured (average of the high and low sensors) temperature and RH, respectively.

Figure 26 shows the simulated temperature and RH results on the interior surface of the XPS and compares them with the measured data. The simulated results stayed within 3.3% and 10.9% of the measured temperature and RH, respectively.

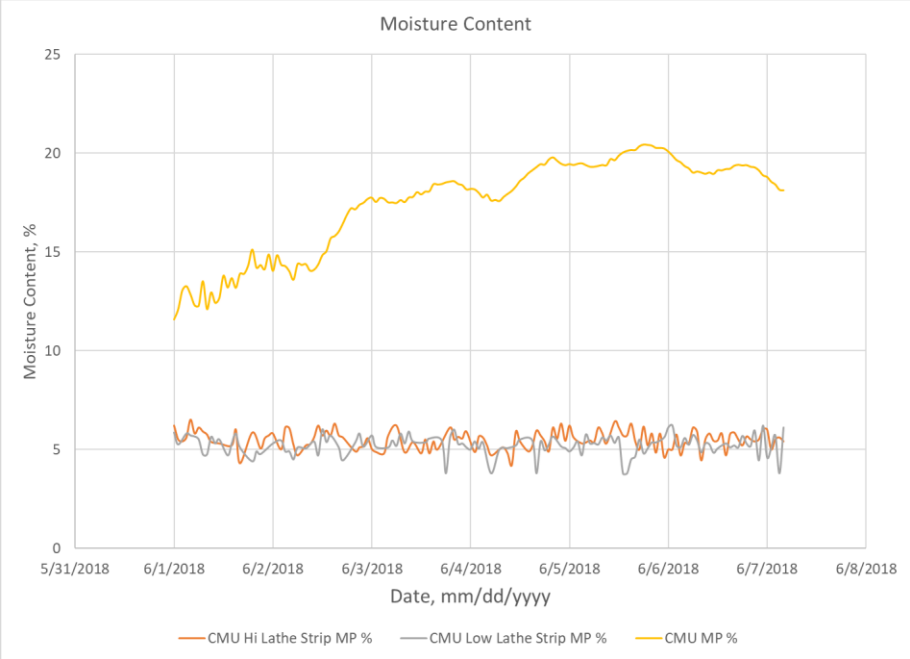

Figure 24. Moisture contents of the wood moisture sensors CM1, CM2, and CM3 (Figure 4).

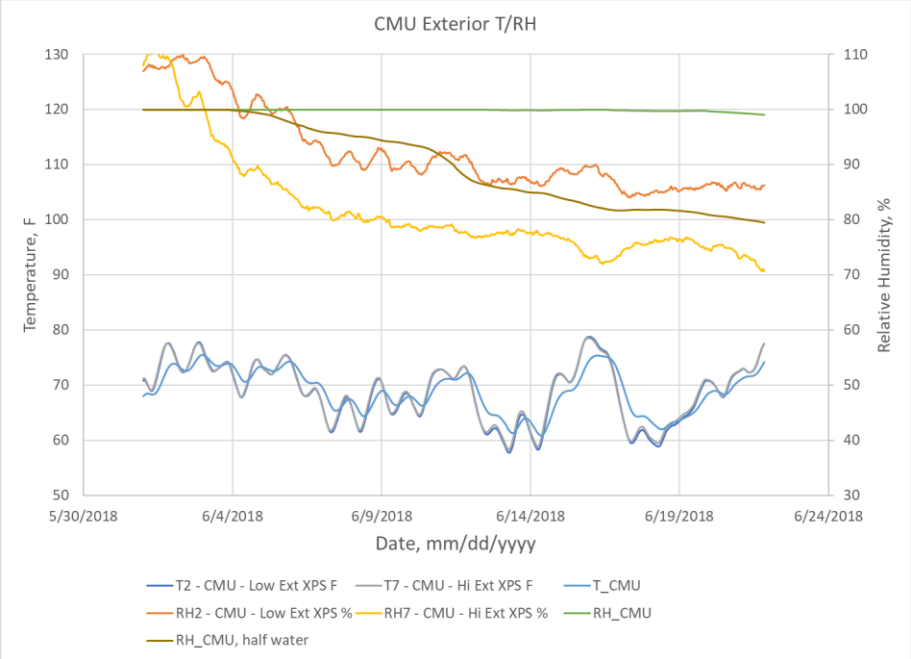

Figure 25. Test runs for CMU wetting on the WRB. Simulations included two levels of added water: Full wetting amount (RH_CMU), and half the injected water (RH_CMU, half water).

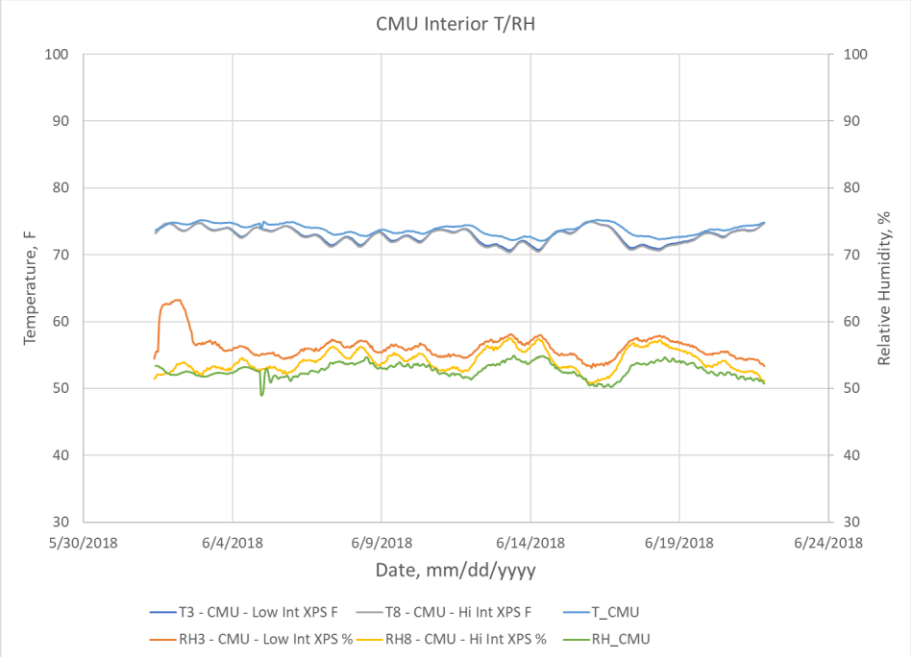

Figure 26. Simulated and measured temperature (T_CMU; T3, T8) and RH (RH_CMU; RH3, RH8) on the interior surface of the XPS (between the XPS and gypsum).

3.2.2 SIP Wall

Figure 27 shows the layer layout for the SIP wall as it was modeled in WUFI. The layers from outside to inside are

1. Vinyl siding
2. Furred air cavity, ¾ in.
3. WRB (spunbonded polyolefin)
4. Air gap, 0.039 in. (mechanically fastened membrane, space for a sensor reading)
5. Low-density fiber glass insulation, 1/8 in., with the initial moisture content equal to the amount of water inserted in the sheet per surface area
6. SIP panel
    a. OSB, 7/16 in.
    b. EPS, 3.6 in.
    c. OSB, 7/16 in.
7. Interior gypsum board, ½ in.

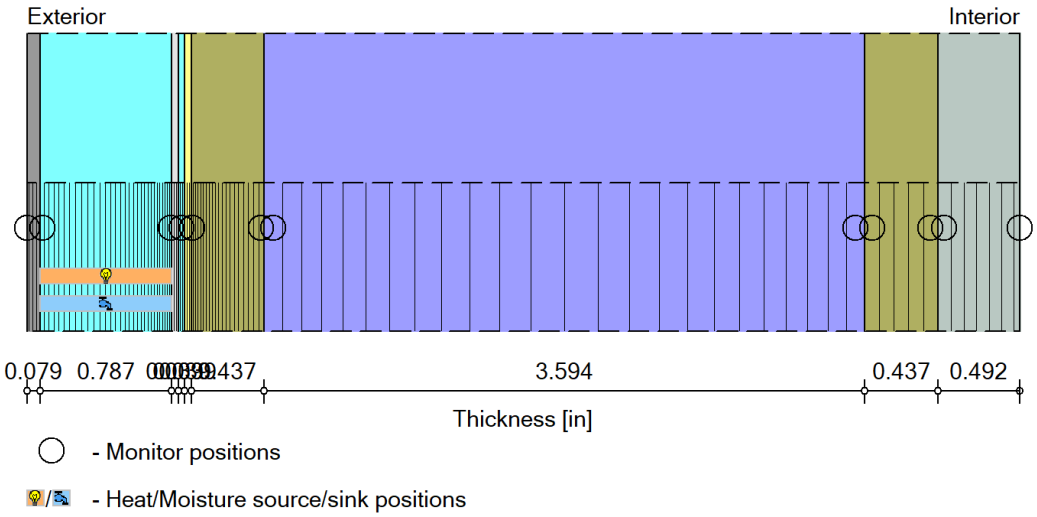

Figure 27. SIP wall assembly as modeled in WUFI with the sorbent sheet between the WRB and exterior OSB in the SIP panel.

The air cavity behind the vinyl siding is vented at air exchange rate of 40 ACH as in previous simulations.

Figure 28 compares the measured and simulated temperature and RH on the exterior side of the WRB in the SIP wall. The simulated results stayed within 21.3% and 37.1% (average of 3.0% and 7.8%) of the measured temperature and RH, respectively. The high discrepancy looks surprising, but the difference is caused by an instantaneous value at a given hour when temperature and RH was changing very quickly. Figure 29 shows the simulated and measured temperatures and the RH between the WRB and SIP panel. The simulated results stayed within 14.1% and 35.7% (average of 2.6% and 6.2%) of the measured temperature and RH, respectively. The large error is caused by the initial drying time taking longer in the simulations than in the measurements. Figure 30 compares the measured and simulated temperature and RH on the interior side of the SIP panel. The simulated results stayed within 4.5% and 6.3% (average of 0.6% and 1.8%) of the measured temperature and RH. Figure 31 compares the measured and simulated moisture content in the exterior half of the OSB layer. The simulation results show slower drying than in the measurements. The sprayed water on the absorbent layer in the measurements initially increased the moisture content of the OSB layer, but the water dried out in half a day. The simulations predict much slower drying out of the OSB layer: the moisture contents and the RH returned to the non-wetted level in about a week.

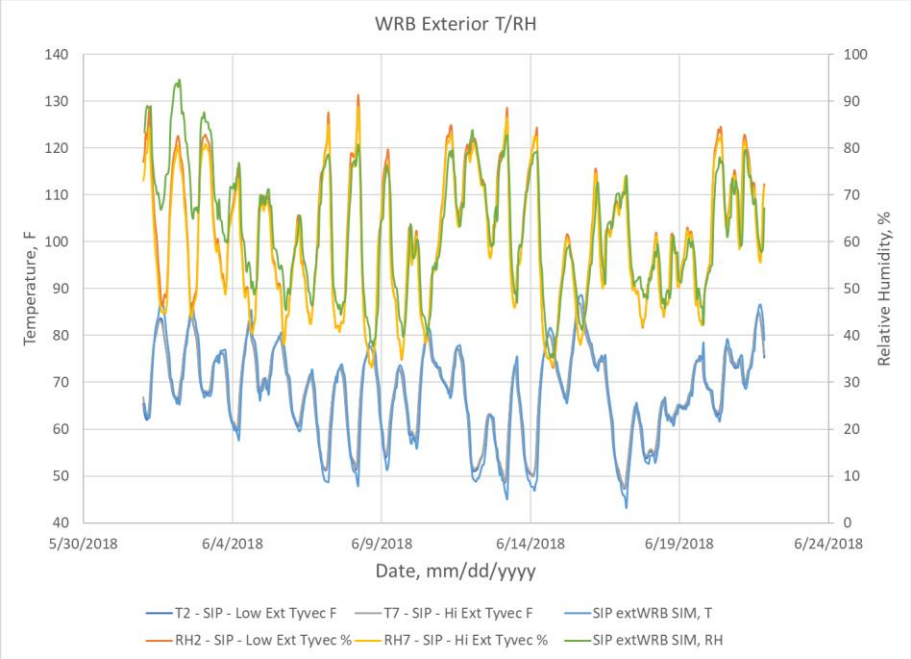

Figure 28. Simulated temperature (SIP extWRB SIM, T) and RH (SIP extWRB SIM, RH) on the exterior side of the WRB. Measured data: Sensors 2 (lower) and 7 (upper) are on the interior side of the OSB in the SIP panel. Summer conditions with only diffusion and wetting.

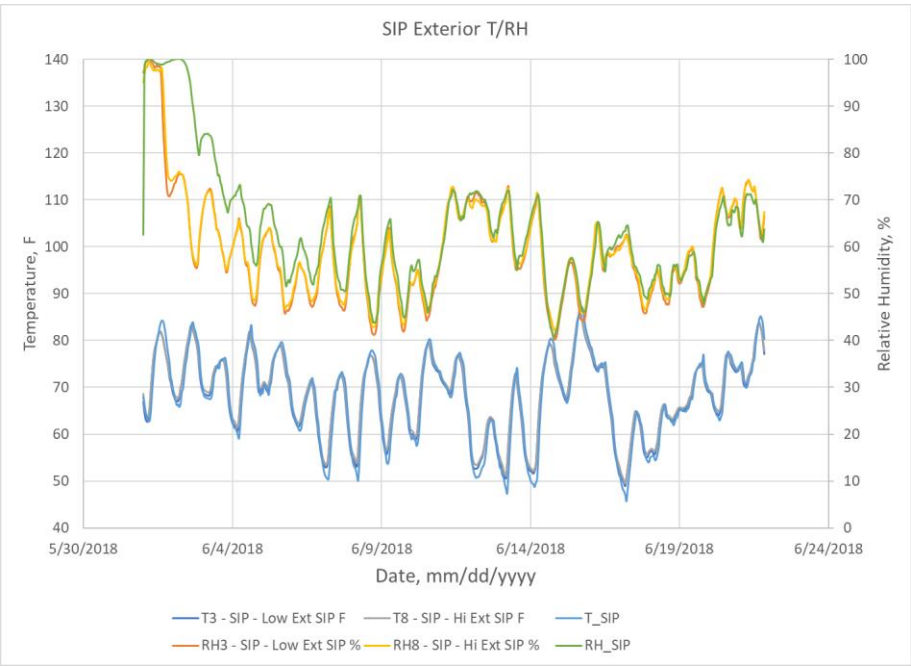

Figure 29. Simulated temperature (T_SIP) and RH (RH_SIP) on the exterior side surface of the SIP panel between the OSB and WRB. Measured data: Sensors 3 (lower) and 8 (upper) are between the OSB and WRB. Summer conditions with only diffusion and wetting.

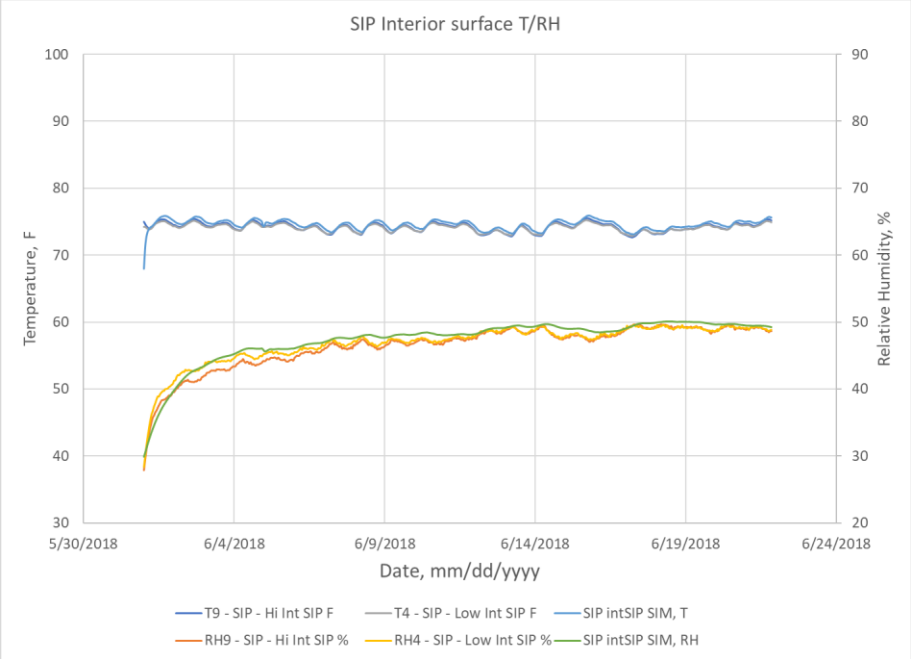

Figure 30. Simulated temperature (SIP intSIP SIM, T) and RH (SIP intSIP SIM, RH) on the interior side surface of the SIP panel. Measured data: Sensors 4 (lower) and 9 (upper) are on the interior side of the OSB in the SIP panel. Summer conditions with only diffusion and wetting.

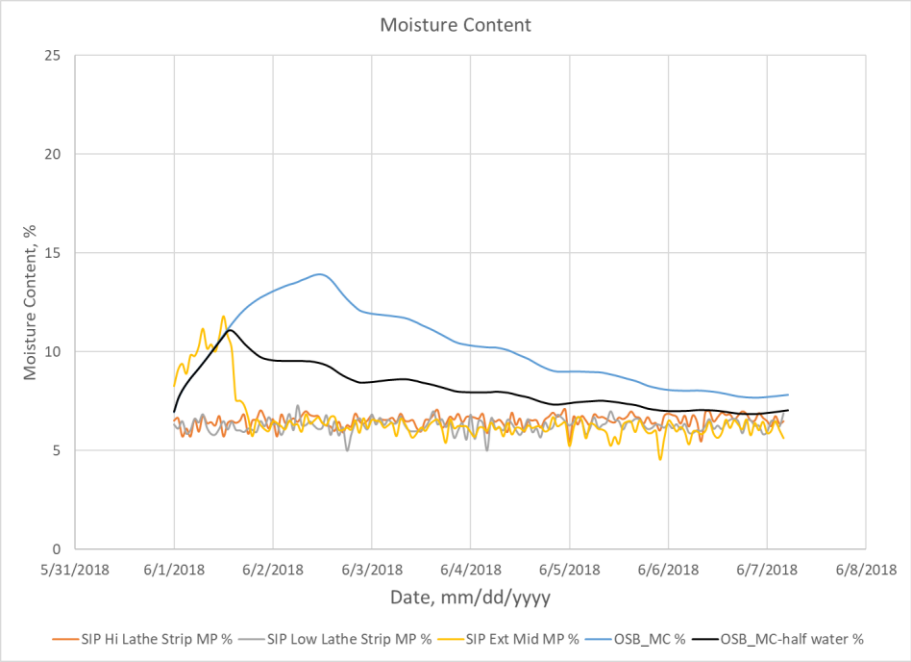

Figure 31. Moisture contents of the wood moisture sensors SM1, SM2 and SM3 (Figure 4) in the wetting test. Simulated results are shown for two initial moisture contents of the absorbent layer: Full amount of water and half the amount of water sprayed on the absorbent layer.

3.3 DIFFUSION AND ADVECTION

To capture the effects of air traveling through the wall, holes were made in each wall to give a pathway for air movement. For the SIP wall, a hole was made along a horizontal seam where the two SIP panels met. The Tyvek and drywall were both cut away to allow unrestricted airflow through the crack shown in Figure 32. The air in the cavity between the lathe strips and behind the vinyl siding was forced through the crack using a pressure difference applied across the wall specimen. The RH and temperature of the air were measured on both sides of the crack, which are shown as blue circles in Figure 32 with sensor labels shown in red.

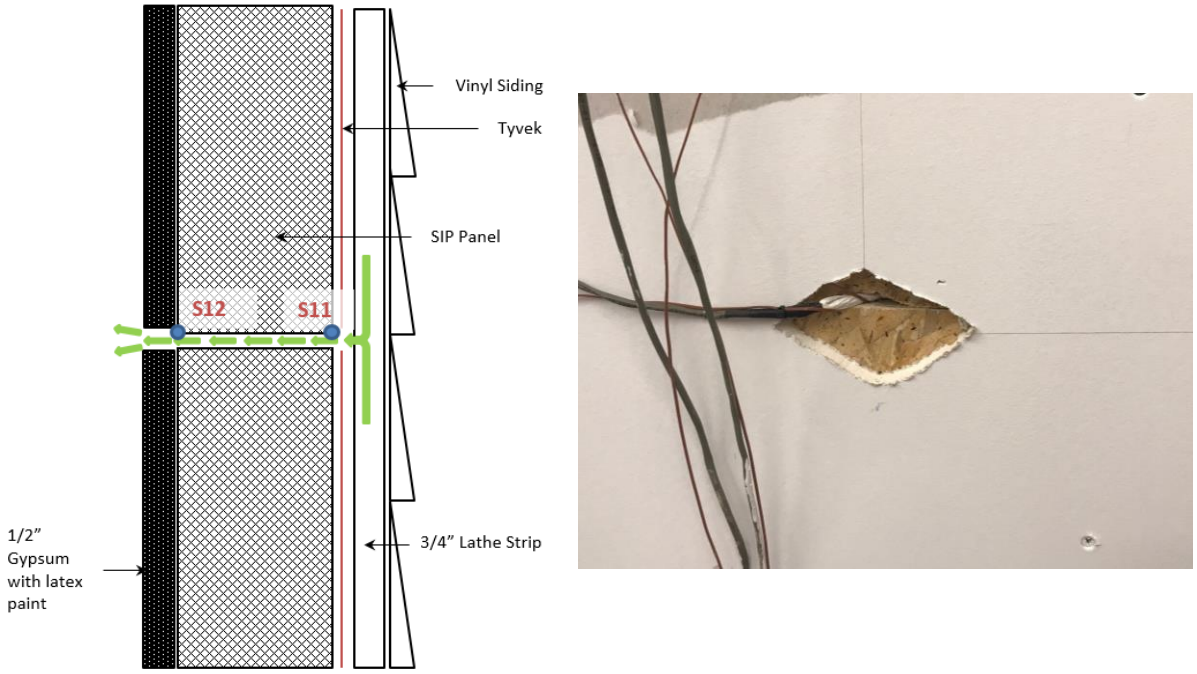

Figure 32. Left: a schematic of the SIP wall with air leak about halfway up the wall. The blue dots indicate new temperature and RH measurements. The green arrows represent the airflow path and direction. Right: a picture of the interior exit of the air leak with temperature and RH sensors seen in the crack.

For the air leak in the CMU wall, three holes with ½ in. diameter were drilled through the mortar between two CMU blocks about halfway up the wall. These holes went through the Sto Gold and XPS layers into the cavity created by the lathe strips. Then, a small hole was cut through the gypsum toward the bottom of the wall so the air could exit as shown in Figure 33. Two new temperature and RH sensors were added to this wall on both sides of the air leak shown as blue dots with labels in Figure 33.

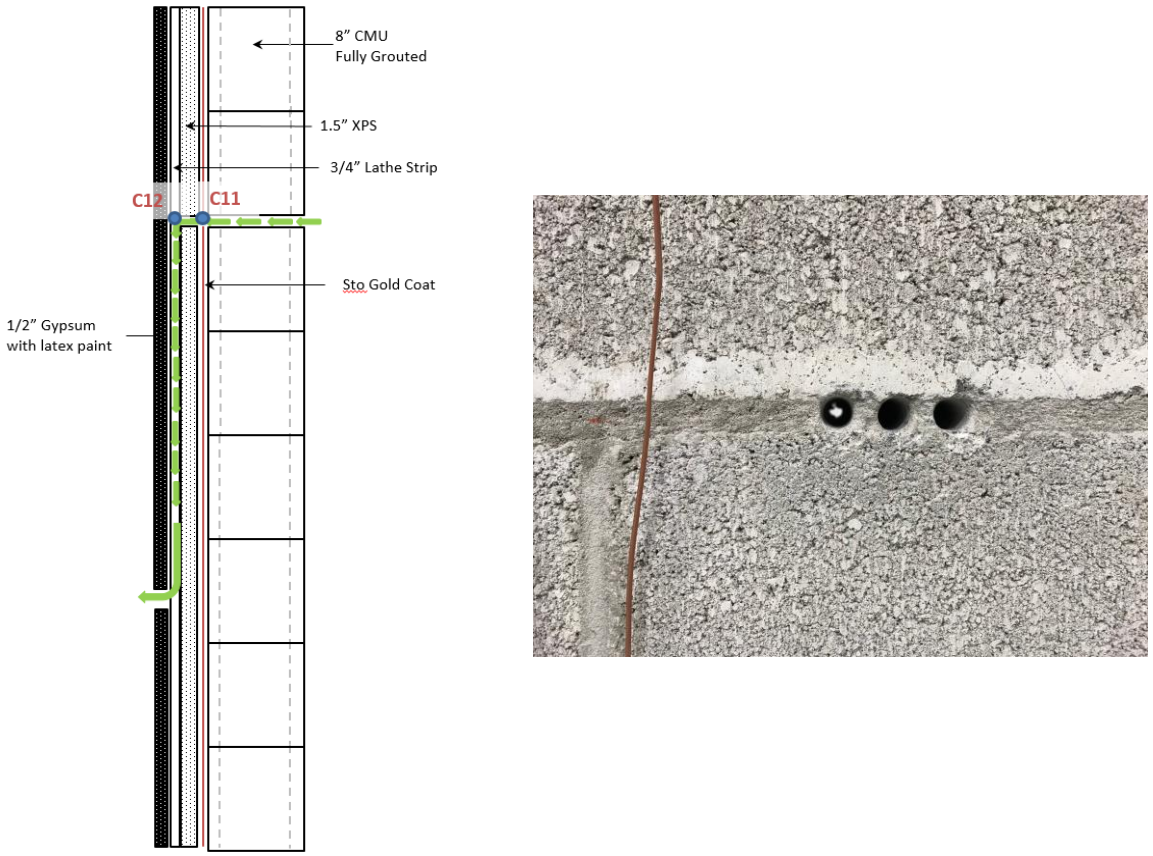

Figure 33. Left: a schematic of the CMU wall with air leak about halfway up the wall. The blue dots indicate new temperature and RH measurements. The green arrows represent the airflow path and direction. Right: a picture of the exterior surface of the CMU wall with the air leak.

To determine the leakage characteristics of the air pathways, the volumetric airflow rate was measured as a function of pressure differential across the wall according to ASTM E283 Standard Test Method before and after the holes were made. The difference between the pre- and post-leak tests yields the leakage characteristics of each air leak path as shown in Figure 34.

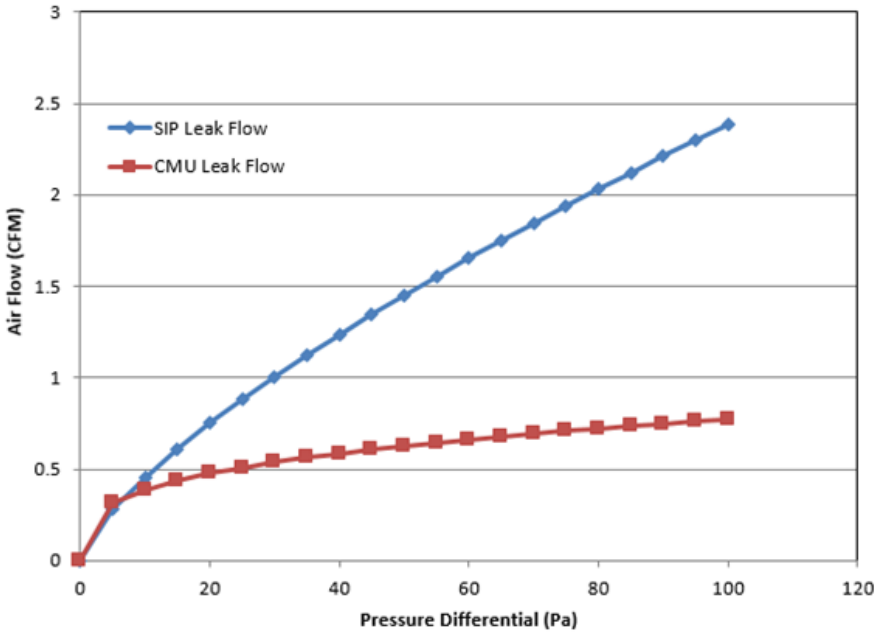

Figure 34. CMU and SIP leakage characteristics.

Chicago summer outdoor weather conditions were followed in the outdoor chamber per Figure 5 and the indoor chamber was set to a constant 75°F at 50% RH. Figure 35 shows the comparison between the outdoor chamber target temperature and RH and what was simulated. Notice that the error is higher than other summer tests, which was caused by the difficulty of maintaining the outdoor climate with a continuous air leak through the wall. During the test, a target 20 Pa pressure difference between the outdoor and indoor chambers was maintained so that outdoor air would infiltrate into the wall. At this pressure, the SIP and CMU walls would have a continuous 0.8 ft^3 and 1.9 ft^3 per minute of air flowing through the leaks, respectively. Figure 36 shows the pressure maintained throughout the test. Notice that there were about 12 hours towards the beginning in which the pressure blower failed and did not supply the needed air to maintain 20 Pa.

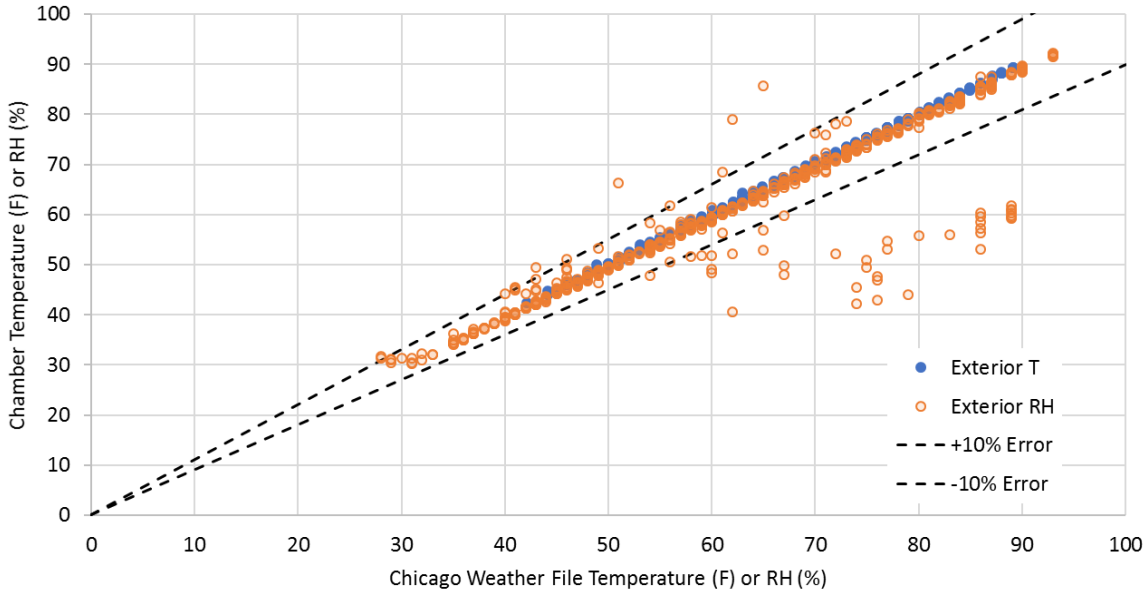

Figure 35. Comparison between the outdoor chamber target temperature and RH and what was simulated for the diffusion and advection experiment.

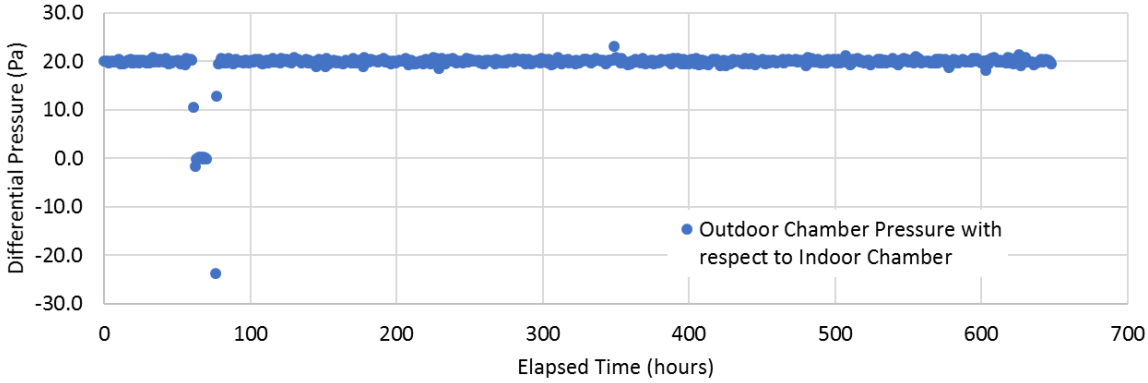

Figure 36. Pressure difference maintained between the outdoor and indoor chambers during the diffusion and advection test.

3.3.1 CMU Wall

WUFI Pro is a one-dimensional hygrothermal simulation model and could not capture airflow along the path of the air leaks through the CMU and the SIP panel walls. However, an attempt was made to evaluate the airflow impact on temperature and RH in the air cavity on the interior side of the CMU wall. The air leak path was a short and direct path in the CMU without any tortuous flow through the materials in the wall. Figure 37 shows the layer layout for the CMU wall as it was modeled in WUFI. The layers from outside to inside are

1. CMU exterior wall
2. Concrete fill
3. CMU interior wall
4. Fluid-applied vapor-permeable air/moisture barrier (Sto Gold Coat TA)
5. XPS, 1.5 in.

6. Furred air cavity, ¾ in. (air exchange rate ACH=40 1/h with air taken directly from outside)
    a. The air layer type in WUFI is “without additional moisture capacity”
7. Interior gypsum board, ½ in.

Simulations were carried out with and without the air leak to evaluate the impact of the airflow on the temperature and RH. The airflow through the leak path was evenly distributed to the volume between the XPS and interior gypsum board.

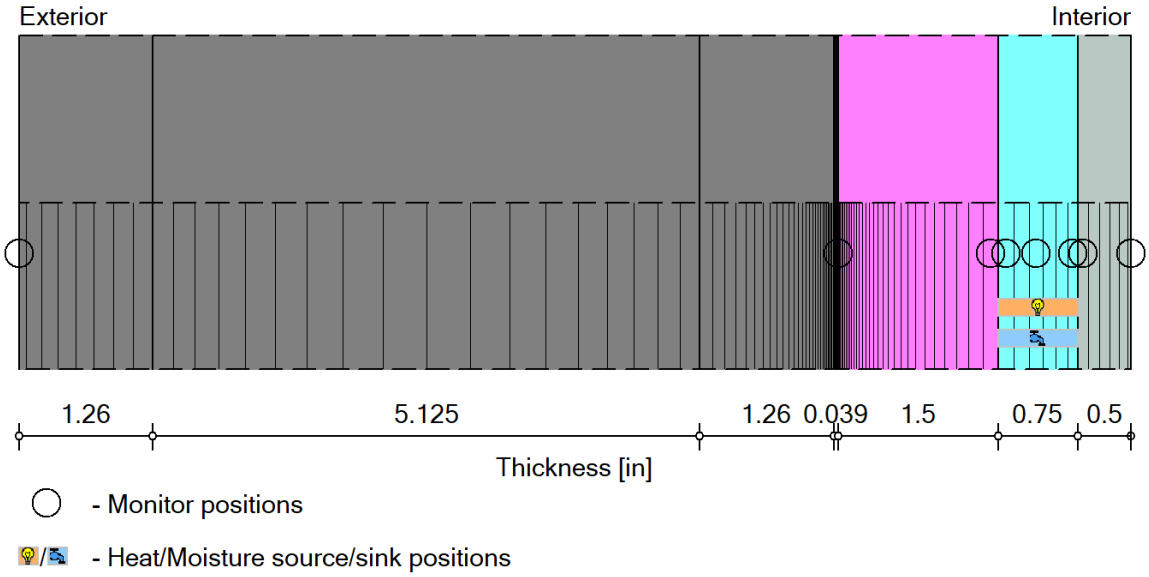

Figure 37. CMU wall assembly as modeled in WUFI with air leakage through the wall modeled by using air exchange from the outside in the air cavity between the XPS and gypsum board.

Figure 38 shows the simulated and measured temperatures and the RH between the XPS and gypsum board. The simulated results stayed within 4.4% and 57.1% (average of 1.8% and 21.9%) of the measured temperature and RH, respectively. The high error >50% in the RH occurred in a short time period in one day. Figure 39 shows the simulated and measured temperatures and the RH between the XPS and air/moisture barrier. The simulated results for the case with no air leakage into the air gap between the XPS and air/moisture barrier stayed within 10.6% and 22.3% of the measured temperature and RH, respectively. When air could leak between the XPS and the air/moisture barrier (1 mm air gap with 300 ACH from the exterior chamber), the simulated results stayed within 4.6% and 25.5% of the measured temperature and RH, respectively. The results show that there was likely an air gap between the XPS and air/moisture barrier, and the air leak did find its way into that gap.

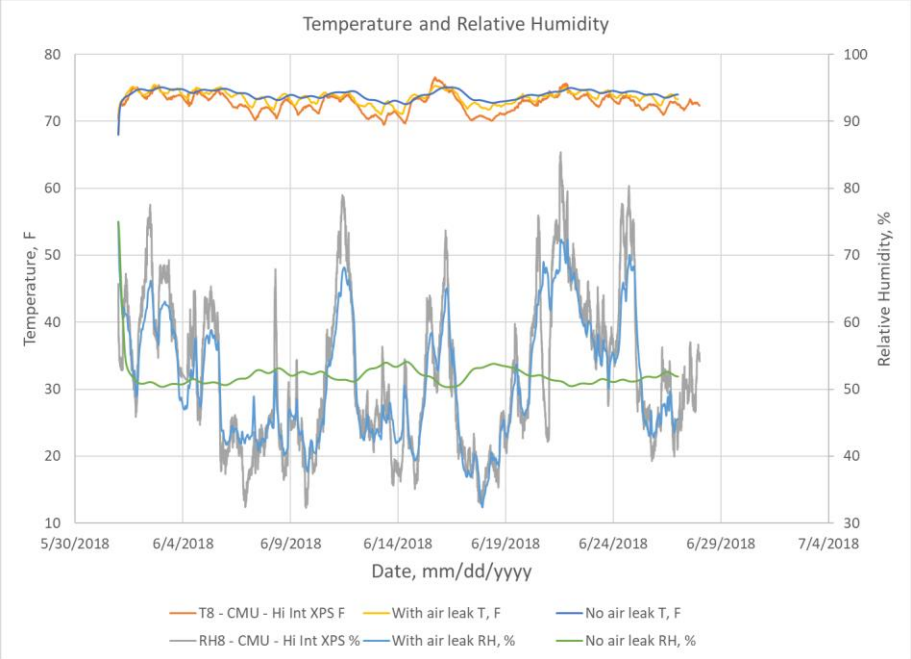

Figure 38. Measured temperature (T8) and RH (RH8) on top part of the air cavity between the gypsum board and XPS with simulated temperature (With/No air leak T, F) and RH (With/No air leak RH, %) in the air cavity when air leakage was present or not.

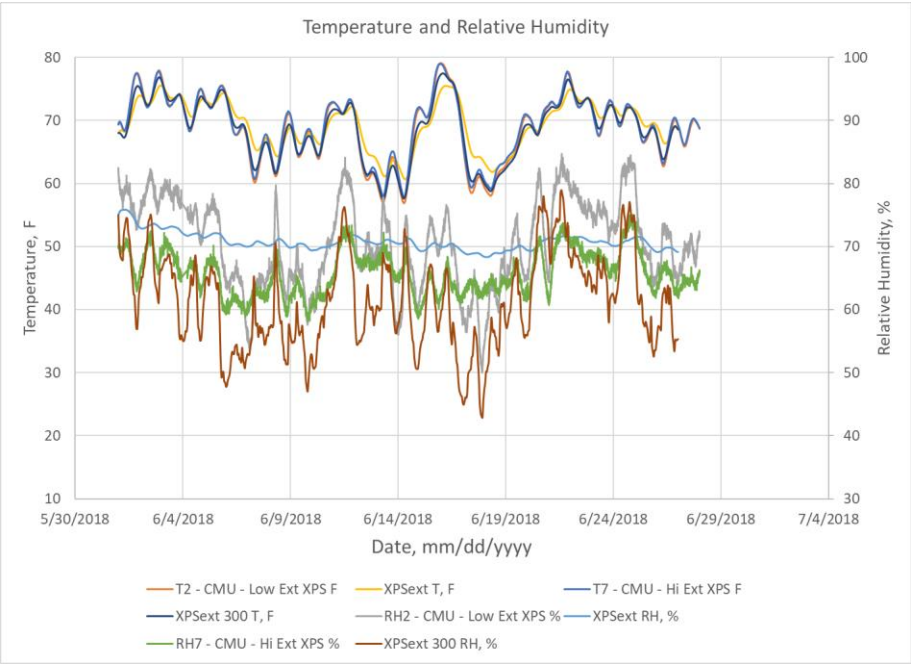

Figure 39. Measured temperature (T2) and RH (RH7) on top and bottom part on the exterior side of the XPS with simulated temperature (XPSext T, F) and RH (XPSext RH, %) when air was not leaking to the gap between the WRB and XPS, and with simulated temperature (XPSext 300 T, F) and RH (XPSext 300 RH, %) when air was leaking to the gap between the WRB and XPS.

Figure 40 shows the difference between the measured temeprature and RH of the leaked air at the interior and exterior sides of the air path through the XPS. Both locations exhibite very similar results, indicating that the leaked air barely affected the temperature or moisture content of the XPS.

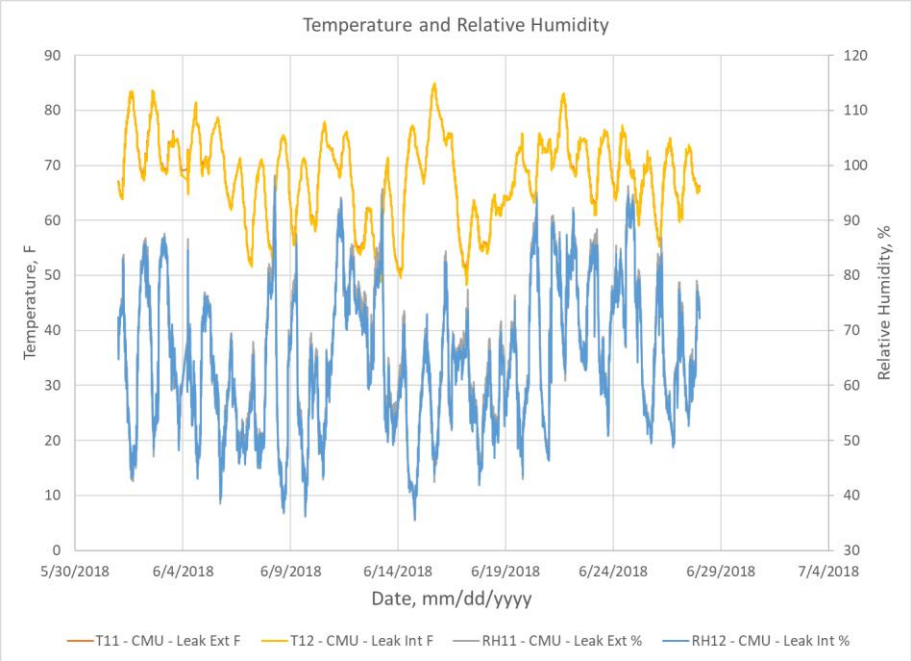

Figure 40. Measured temperature (T11) and RH along the airflow path on the exterior side (RH11) and on the interior side (T12, RH12) of the XPS in the CMU wall.

3.3.2 SIP Wall

WUFI Pro is a one-dimensional hygrothermal simulation model and could not capture airflow along the path of the air leaks through the CMU and SIP panel walls. However, an attempt was made to evaluate the airflow impact on temperature and RH in the air cavity on the interior side of the SIP wall. Simulations were carried out with and without the air leak to evaluate the impact of the airflow on the temperature and RH. The airflow through the leak path was evenly distributed to the volume between the OSB in the SIP panel and the interior gypsum board. The air mostly bypassed the layers in the wall and flowed directly into the indoor room without first spreading into an air cavity as it did in the CMU wall. To capture the effect in the simulations, a 0.1 in.-thick air layer (full wall height) was added between the gypsum board and SIP panel. This air cavity was ventilated with the air from the outdoor chamber at the air leakage rate. Another simulation was carried out to increase the local impact by assuming the air gap to be only about 5 in. tall, thus increasing the air exchange rate by 20 times. Figure 41 shows the layer layout for the SIP wall as it was modeled in WUFI. The layers from outside to inside are

1. Vinyl siding
2. Furred air cavity, ¾ in.
3. WRB (spunbonded polyolefin)
4. Air gap, 0.039 in. (mechanically fastened membrane, space for a sensor reading)
5. Low-density fiber glass insulation, 1/8 in
6. SIP panel
    a. OSB, 7/16 in.
    b. EPS, 3.6 in.
    c. OSB, 7/16 in.

8. Air cavity (varying air exchange rates)
    d. The air layer type in WUFI is “without additional moisture capacity”
7. Interior gypsum board, ½ in.

Figure 42 shows the simulated and measured temperatures and the RH on the exterior side of the WRB in the SIP wall. The simulated results stayed within 2.2% and 10.2% of the measured temperature and RH, respectively. Figure 43 shows the simulated and measured temperatures and the RH on the exterior side of the SIP panel in the SIP wall. The simulated results stayed within 2.7% and 11.6% of the measured temperature and RH, respectively. Figure 44 shows the simulated and measured temperatures and the RH on the interior side of the SIP panel in the SIP wall. The simulated results stayed within 0.5% and 4.7% of the measured temperature and RH, respectively.

Figure 45 shows the simulated temperature and RH in the air cavity between the gypsum board and SIP panel with two different air exchange rates and compares the results with the measured values in which air entered the indoor chamber from the wall. Figure 46 illustrates that the temperature and the RH of the air entering the wall from the outdoor chamber and exiting the wall to the indoor chamber are almost the same throughout the measurement period. The air passed through the wall without much heat or moisture exchange with the wall.

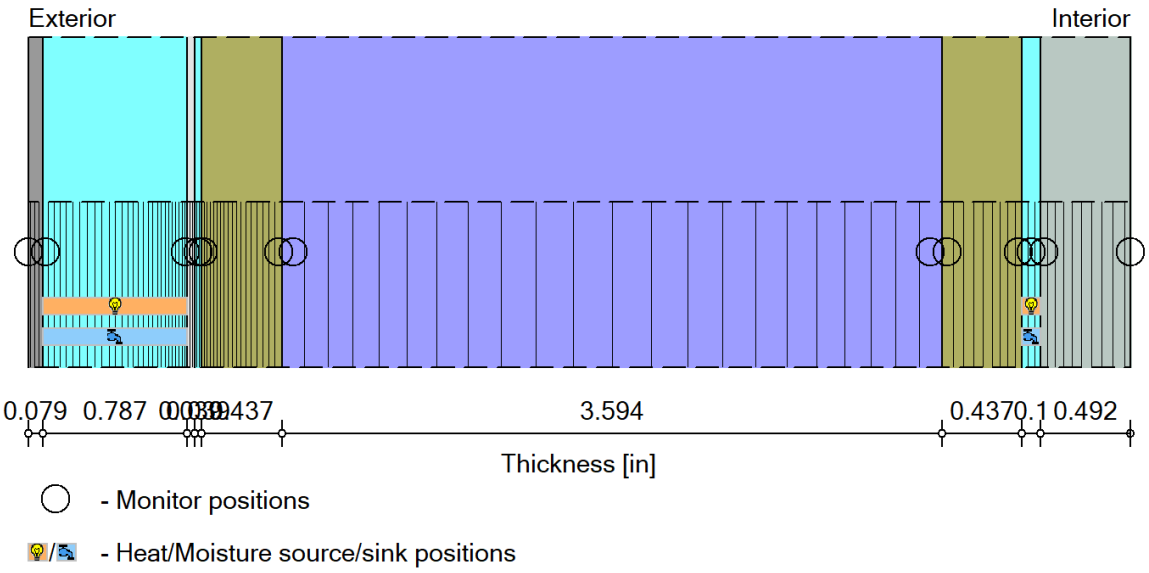

Figure 41. SIP wall assembly as modeled in WUFI with the airflow exchange from the exterior side to the gap between the SIP panel and interior gypsum board.

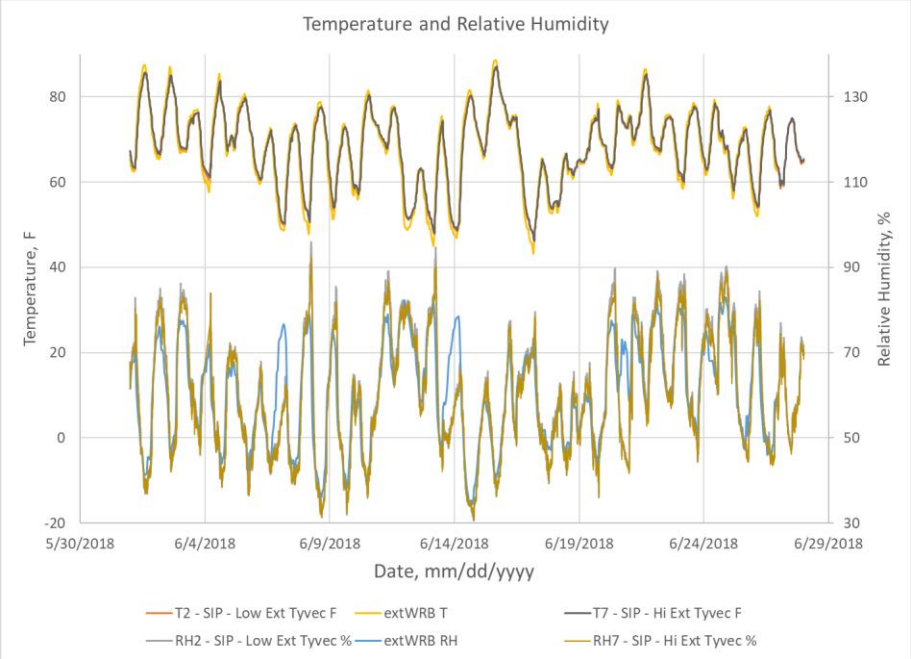

Figure 42. Simulated temperature (extWRB T) and RH (extWRB RH) on the exterior side surface of the WRB. Measured data: Sensors 2 (lower) and 7 (upper) are on the exterior side of WRB in the SIP panel. Summer conditions with air leakage through the wall.

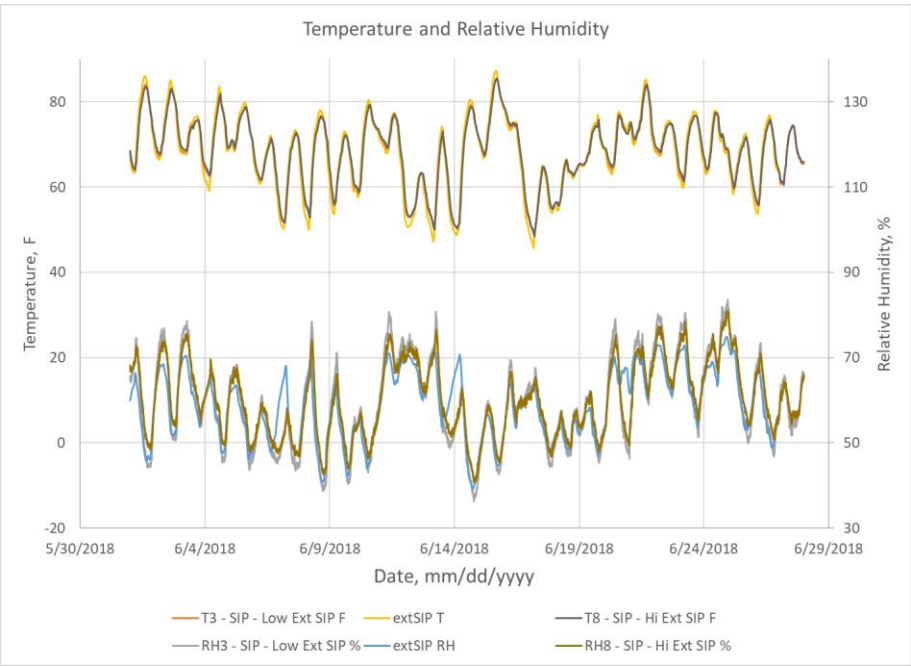

Figure 43. Simulated temperature (extSIP T) and RH (extSIP RH) on the exterior side surface of the SIP panel. Measured data: Sensors 3 (lower) and 8 (upper) are on the exterior side of the SIP panel. Summer conditions with air leakage through the wall.

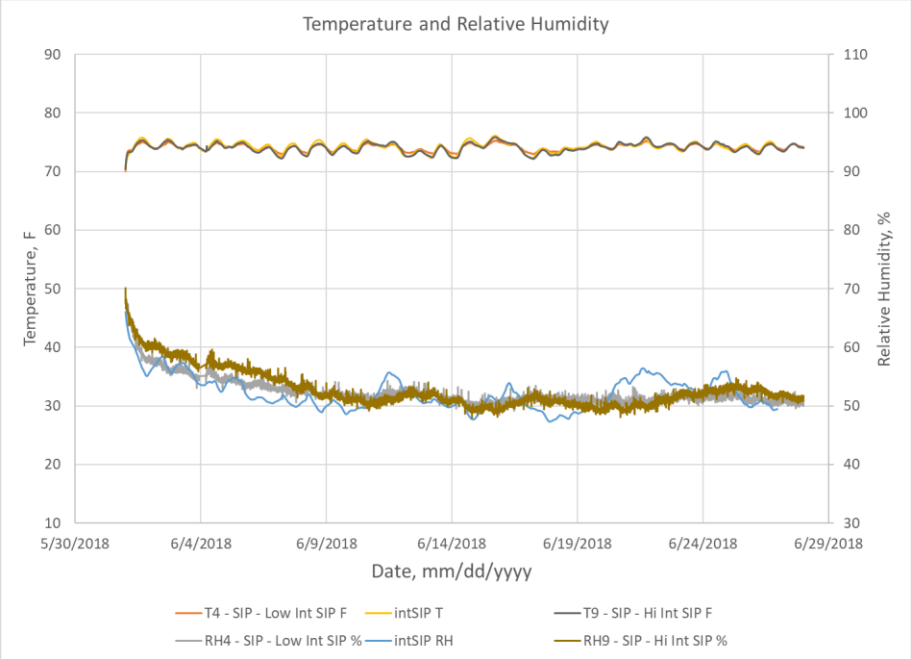

Figure 44. Simulated temperature (intSIP T) and RH (intSIP RH) on the interior side surface of the SIP panel. Measured data: Sensors 4 (lower) and 9 (upper) are on the exterior side of the SIP panel. Summer conditions with air leakage through the wall.

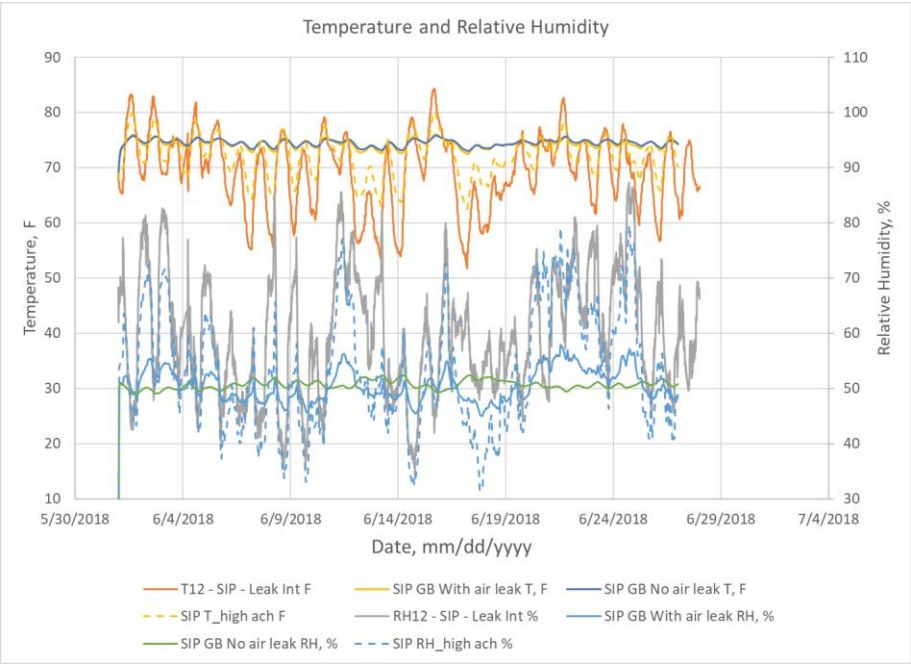

Figure 45. Measured temperature (T12) and RH (RH12) between the gypsum board and OSB with simulated temperature (With/No air leak T, F) and RH (With/No air leak RH, %) in the air cavity when air leakage was present or not. Dashed lines are for a case that had very high air exchange from the outside in the 0.1 in.-thick cavity between the gypsum board and SIP panel.

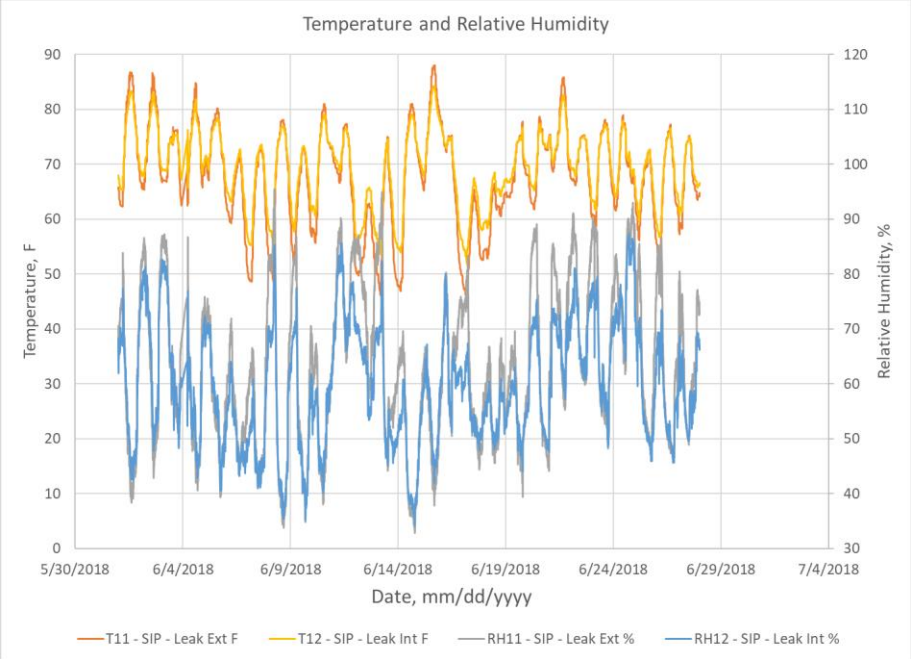

Figure 46. Measured temperature (T11) and RH (RH11) along the airflow path on the exterior side and on the interior side of the SIP panel (T12, RH12).

3.4 DIFFUSION, ADVECTION, AND SOLAR-DRIVEN MOISTURE

For the final test, solar-driven moisture was added to the modes of moisture transfer that were tested in the chamber. This test focused on the CMU wall. The weather conditions and differential pressure that were simulated were the same as the previous diffusion and advection test. To determine how much solar insolation would be needed to be an incident on the wall, an Energy Plus simulation was run to find the surface temperature of the south-facing façade of a residential home in Chicago for the summer months. All the outdoor chamber control targets for this test are shown in Figure 47. This simulation was used as the target for controlling the light rack intensity, which uses thermocouples on the wall surface in a closed loop control system to maintain the target surface temperature of the CMU wall.

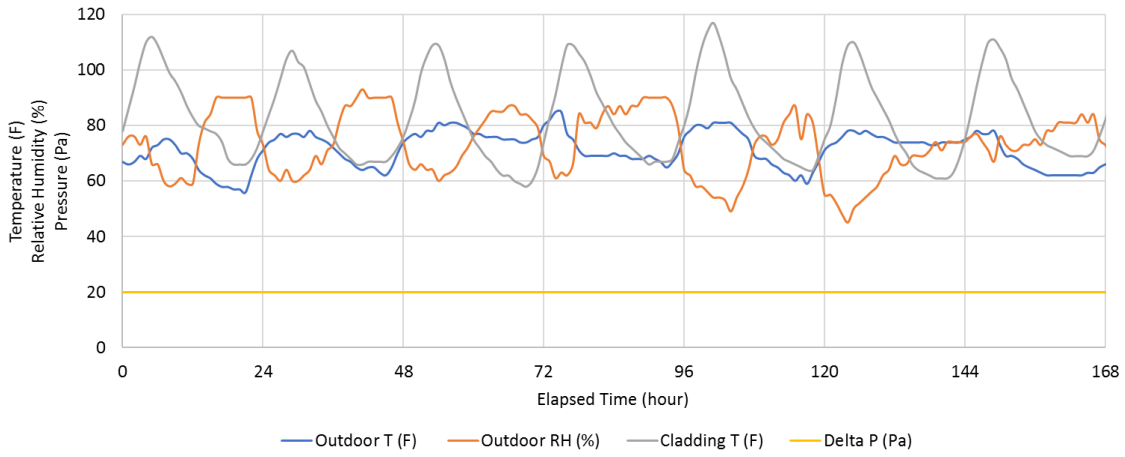

Figure 47. Outdoor chamber targets for diffusion, advection, and solar-driven moisture test.

To facilitate solar-driven moisture, a large section of the CMU was wetted with water using a spray bottle for four consecutive mornings. Table 6 shows the time and mass of water added, and Figure 48 shows the wet CMU wall behind the solar rack in the chamber.

Table 6. Time and mass of water added to the exterior surface of the CMU wall each day of the test.

Day	Time (Chicago-correlated)	Mass of water misted on CMU (g)
1 (July 27)	7:45 AM	269
2	8:00 AM	245
3	8:00 AM	279
4	7:30 AM	244

Figure 48. Exterior of the CMU wall shown wet with solar rack in front of wall. The wetted area was 30 in. wide and 48 in. tall and was centered on the wall.

Figure 49 and Figure 50 show how well the conditions in the chamber were maintained compared to the target during the diffusion, advection, and solar-driven moisture experiment.

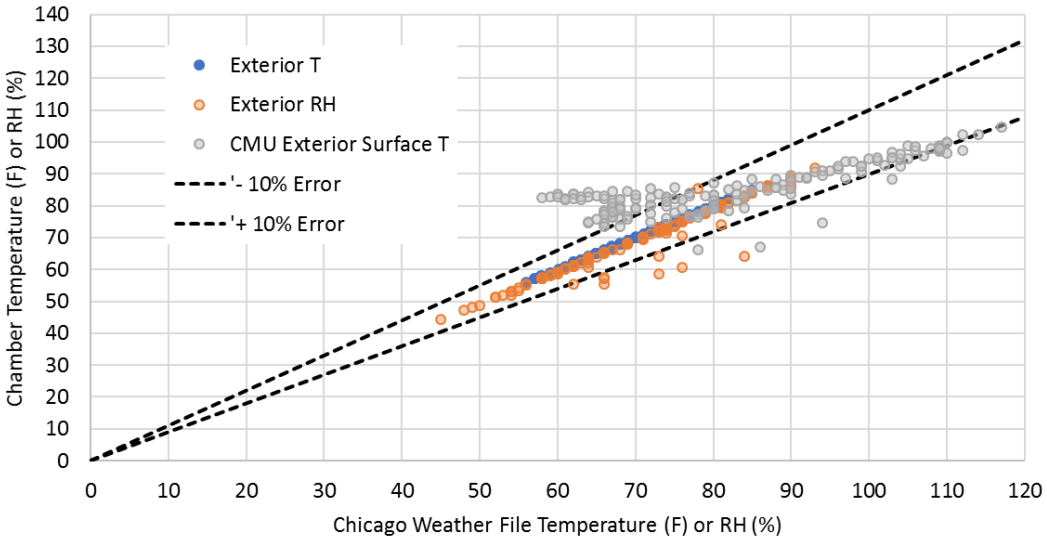

Figure 49. Comparison between the outdoor chamber target temperature and RH and what was simulated for the diffusion, advection, and solar-driven moisture experiment.

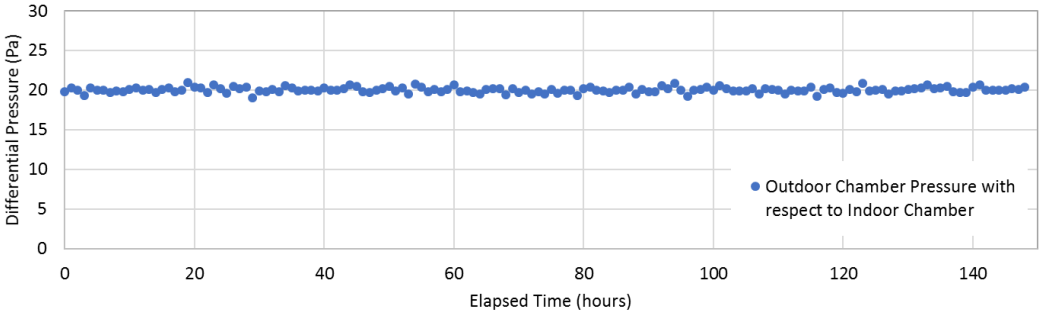

Figure 50. Pressure difference maintained between the outdoor and indoor chambers during the diffusion, advection, and solar-driven moisture test.

3.4.1 CMU Wall

The weather conditions for hygrothermal simulations were created by first running WUFI for the wall design (Figure 51) with the TMY3 weather file for Chicago by facing the wall south. The resulting solar radiation intensity on the wall in WUFI was output to create the hourly solar radiation boundary condition for the subsequent calculations. WUFI weather file type “kli” was created by taking this hourly solar radiation as “measured” solar radiation on the wall. The temperature and RH in both the exterior and the interior chamber were used for ambient conditions, and finally, the wetting events (Table 6) in unit mass per wetted wall surface area (30 in. × 46 in.) were used as “measured rain” on the wall at 8:00 AM in the first four days. The simulations were run with 1 h time intervals.

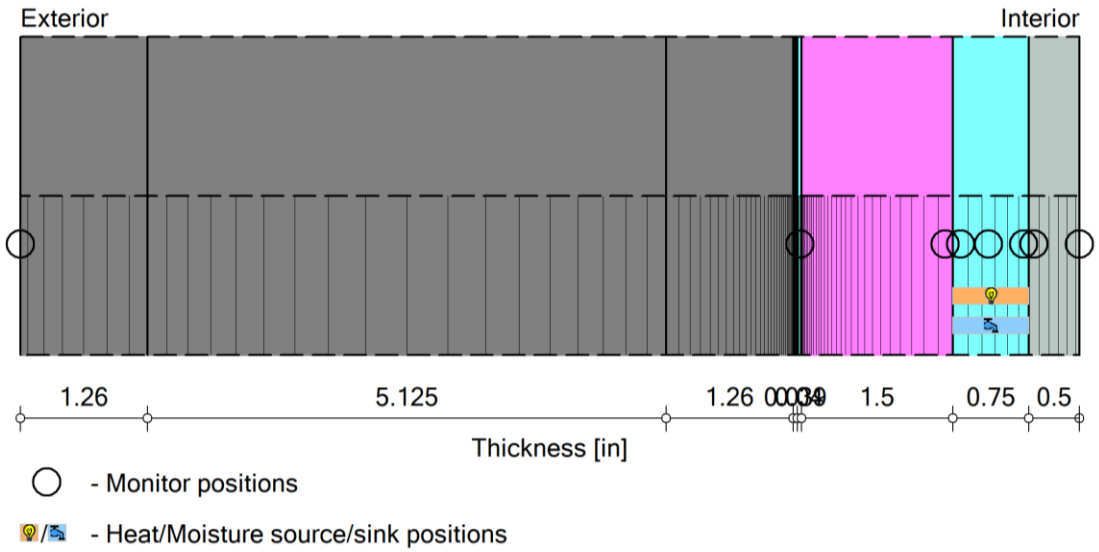

Figure 51. CMU wall structure as modeled in WUFI for diffusion, advection, and solar-driven moisture test.

Figure 52 shows the simulated and measured temperatures and RH on the lower part of the exterior surface of the CMU and between the air/moisture barrier and XPS. The simulated results for the air/moisture barrier and XPS interface stayed within 7.6% and 16.2% (average of 3.1% and 7.4%) of the measured temperature and RH, respectively. The simulated results for the exterior surface stayed within 12.7% and 50.7% (average of 3.5% and 13.5%) of the measured temperature and RH, respectively. The high discrepancy in RH was caused by a short spike in a day. The exterior surface temperature and RH followed the trends well.

Figure 53 shows the same comparison as Figure 52 but for the upper part of the CMU wall. This part experienced higher temperatures on the exterior surface than the lower part of the CMU wall because of warm air rising from the surface of the wall, which could not be considered in the one-dimensional WUFI simulation. The simulated results for the air/moisture barrier and XPS interface stayed within 6.9% and 19.5% (average of 2.5% and 9.4%) of the measured temperature and RH, respectively. The simulated results for the exterior surface stayed within 18.7% and 54.2% (average of 5.6% and 16.5%) of the measured temperature and RH, respectively.

In the CMU wall, the simulated results stayed within 7.2% and 11.5% of the measured temperature and RH between the air/moisture barrier and XPS, respectively. The simulated results for the exterior surface stayed within 15.7% and 52.5% of the measured temperature and RH, respectively.

Figure 54 shows the simulated and measured temperatures and the RH on the interior surface of the XPS. The simulated results stayed within 1.8% and 18.1% of the measured temperature and RH, respectively.

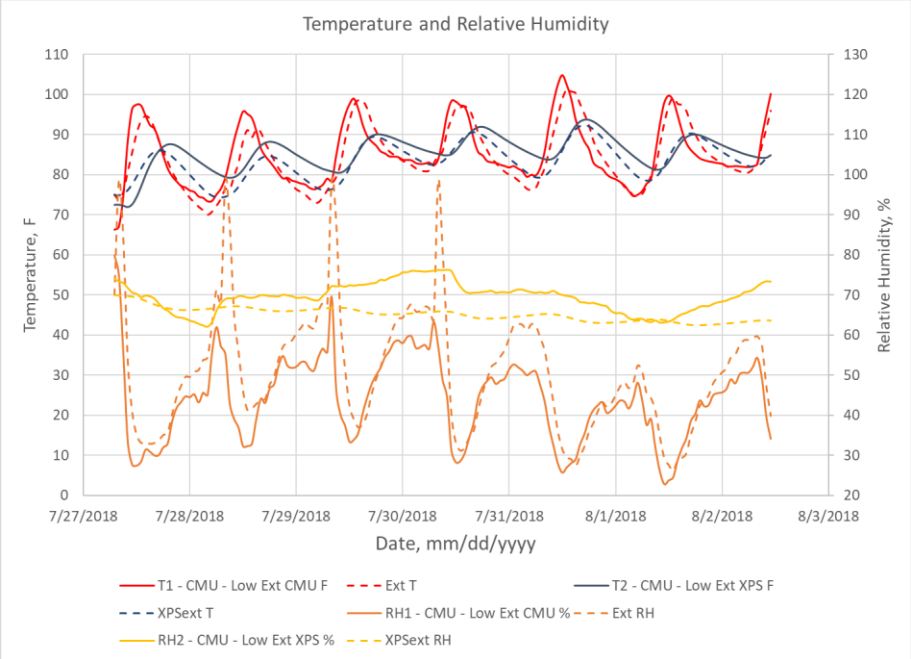

Figure 52. Measured temperature (T1) and RH (RH1) on the lower part of the exterior surface on the CMU block, and between the air/moisture barrier and XPS (T2, RH2). Simulated temperature and RH in the same locations ("XPSext T" and "XPSext RH" are temperature and RH between the air/moisture barrier and XPS, and "Ext T" and "Ext RH" are the simulated temperature and RH on the exterior surface, respectively).

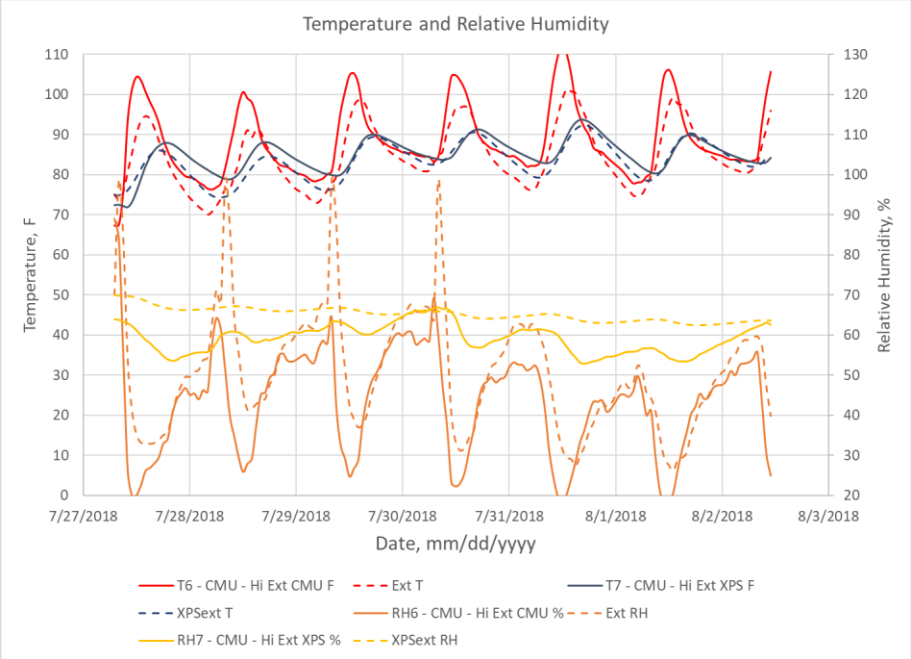

Figure 53. Measured temperature (T1) and RH (RH1) on the upper part of the exterior surface on the CMU block, and between the air/moisture barrier and XPS (T2, RH2). Simulated temperature and RH in the same locations ("XPSextT" and "XPSext RH" are temperature and RH between the air/moisture barrier and XPS, and "Ext T" and "Ext RH" are temperature and RH on the exterior surface, respectively).

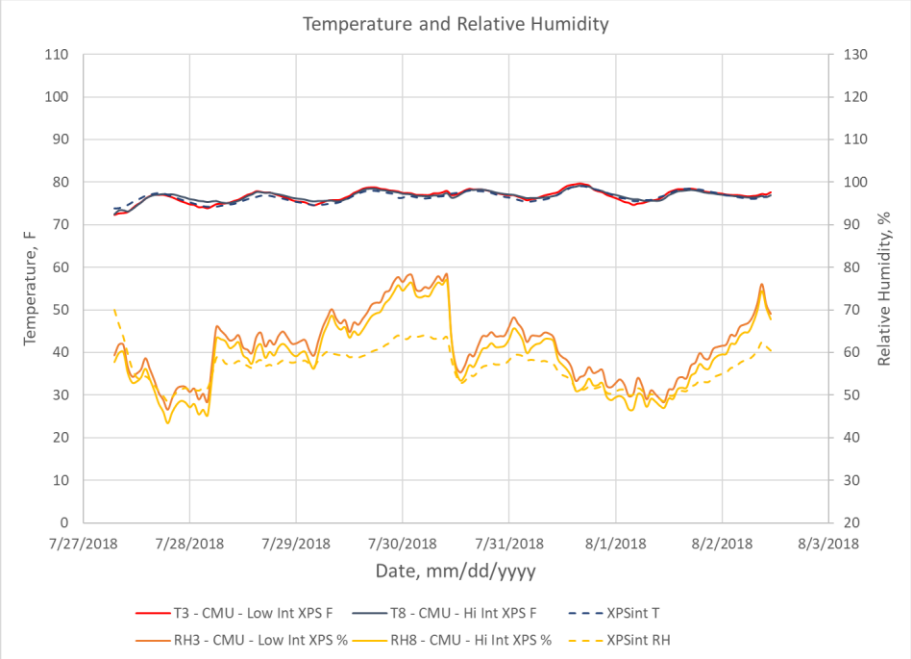

Figure 54. Measured temperature (T3, T8) and RH (RH3, RH8) on the interior surface on the XPS, and simulated temperature (XPSint T) and RH (XPSint RH) in the same locations.

WUFI simulations are one-dimensional and the height of the wall does not play a role in the results. In the measured data, however, the upper part has higher temperatures than the bottom part on the exterior surface because of radiation heat rising from the warm surface. The measured and simulated temperatures have a larger difference in the upper part of the wall (Figure 53) than in the lower part (Figure 52). The measured RH between the air/moisture barrier and XPS was higher than the measured value in the lower part of the wall, and the measured RH in the upper part of the wall was lower than the simulated value.

The materials in the CMU block wall for the masonry construction were not characterized with any measured data in the laboratory. CMU blocks come in different densities and types, and their material properties—including thermal conductivity, thermal capacity, and moisture properties—can significantly vary. The cavities in the CMU block were filled with concrete. Similarly, concrete can have very different compositions and curing rates, and the properties vary over times when curing occurs.

4. CONCLUSION

The main purpose of this work was to demonstrate confidence in the authors' WUFI simulations by comparing simulation results with measured hygrothermal wall performance in an environmental chamber. Experiments were completed with the moisture transport phenomenon of diffusion, bulk moisture intrusion, advection, and solar-driven moisture. Table 7 and Table 8 show the maximum percentage differences in each experiment between measured and simulated results for key measurement locations of temperature and RH. As noted in Section 3, average percentage differences were typically much lower than the maximum differences, which usually occurred over a short time in the test.

Table 7. Maximum percentage difference between measured and simulated performance of the CMU wall at key locations for temperature (T) and RH.

Test and season for CMU wall	XPS interior surface		XPS exterior surface	
	T (%)	RH (%)	T (%)	RH (%)
Diffusion				
Summer	1.1	10.0	3.9	11.2
Winter	8.1	8.1	2.2	1.8
Bulk moisture				
Summer	3.3	10.9	10.5/10.6*	26.8/12.9*
Diffusion and advection				
Summer	4.4	57.1	10.6	22.3
Diffusion, advection, and solar-driven moisture				
Summer	1.8	18.1	7.2	11.5

*Half of water

Table 8. Maximum percentage difference between measured and simulated performance of the SIP wall at key locations for temperature (T) and RH.

Test and season for SIP wall	SIP interior surface		SIP exterior surface		WRB exterior side	
	T (%)	RH (%)	T (%)	RH (%)	T (%)	RH (%)
Diffusion						
Summer	3.3	2.4	8.2	24.4	9.7	25.6
Winter	4.0	11.3	16.7	11.9	17.8	15.7
Bulk moisture						
Summer	4.5	6.3	14.1	35.7	21.3	37.1
Diffusion and advection						
Summer	0.5	4.7	2.7	11.6	2.2	10.2

Other conclusions from this work include

1. Errors between measured and simulated values decreased as measurements got closer to the interior side of the wall.
2. Phenomenon including liquid water caused large discrepancies between measurement and simulation results. Simulated results showed slower drying of materials than measured results.
3. The one-dimensional nature of WUFI Pro made simulating air leaks difficult.
4. The air leaks that were intentionally made in these walls did not affect the materials. The flow rates were too high and would be better characterized as “energy leaks” than “moisture leaks” (Künzel, Zirkelbach, and Scfafaczek 2011).

5. REFERENCES

"2009 IECC Cost Effective Analysis." In. 2012. 400 Prince George's Blvd: NAHB Research Center.

"2012 IECC Cost Effective Analysis." In. 2012. Upper Marlboro MD: NAHB Research Center.

ASHRAE. 2016. "ANSI/ASHRAE Standard 160-2016 Criteria for Moisture-Control Design Analysis in Buildings." In. Atlanta, GA: America Society of Heating, Refrigeration and Air-Conditioning Engineers.

DOE. 2014. "Windows and Building Envelope Research and Development: Roadmap for Emerging Technologies." In.: U.S. Department of Energy - Buildings Technologies Office.

"High-R Walls." In. 2013. *Building America Top Innovations Hall of Fame Profile*, 2. DOE Building Technologies Program.

Holm, Andreas, and Hartwig Kunzel. 1999. "Combined effect of temperature and humidity on the deterioration process of insulation materials in ETICS." In *5th Symposium on Building Physics in the Nordic Countries*, 677-84. Göteborg.

IBP, Fraunhofer. "Wufi - Software for calculating the coupled heat and moisture transfer in building components." http://www.wufi.de/index_e.html.

Künzel, H.M., D. Zirkelbach, and B Scfafaczek. 2011. Vapour control design in wooden structures including moisture sources due air exfiltration. Paper presented at the 9th Nordic Symposium on Building Physics - NSB 2011, Tampere, Finland.

Kunzel, Hartwig. 1995. "Simultaneous heat and moisture transport in building components—One- and two-dimensional calculations using simple parameters." In *IRB Verlag*

Kunzel, Hartwig, and K. Kiebl. 1996. "Drying of brick walls after impregnation." In *Internationale Zeitschrift für Bauinstandsetzen 2*, 87-100.

Kunzel, Hartwig, K. Kiebl, and M. Krus. 1995. "Moisture in exposed building components." In *International symposium on moisture problems in building walls*, 258-65. Porto.

Lstiburek, J., K. Ueno, and S. Musunuru. 2016. "Modeling Enclosure Design in Above-Grade Walls." In. United States: N.p.

Mendon, VW, A Selvacanabady, M Zhao, and ZT Taylor. 2015. "National Cost Effectiveness of the Residential Provisions of the 2015 IECC." In.: Pacific Northwest National Laboratory.

Viitanen, H.A., M. Krus, T. Ojanen, V. Eitner, and D. Zirkelbach. 2015. Mold Risk Classification Based on Comparative Evaluation of Two Established Growth Models. Paper presented at the 6th International Building Physics Conference, IBPC 2015.

APPENDIX A.

WUFI Pro 6.3

Material: *CMU block

Property	Unit	Value
Bulk density	[lb/ft³]	138.278
Porosity	[ft³/ft³]	0.123
Specific Heat Capacity, Dry	[Btu/lb°F]	0.203
Thermal Conductivity, Dry, 50°F	[Btu/h ft°F]	9.2400E-1
Permeability	[perm in]	0.605
Reference Water Content	[lb/ft³]	4.807
Free Water Saturation	[lb/ft³]	7.679
Water Absorption Coefficient	[lb/in²s^0.5]	2.50000E-5
Moisture-dep. Thermal Cond. Supplement	[%/M.-%]	8
Temp-dep. Thermal Cond. Supplement	[Btu/h ft°F²]	6.40000E-5

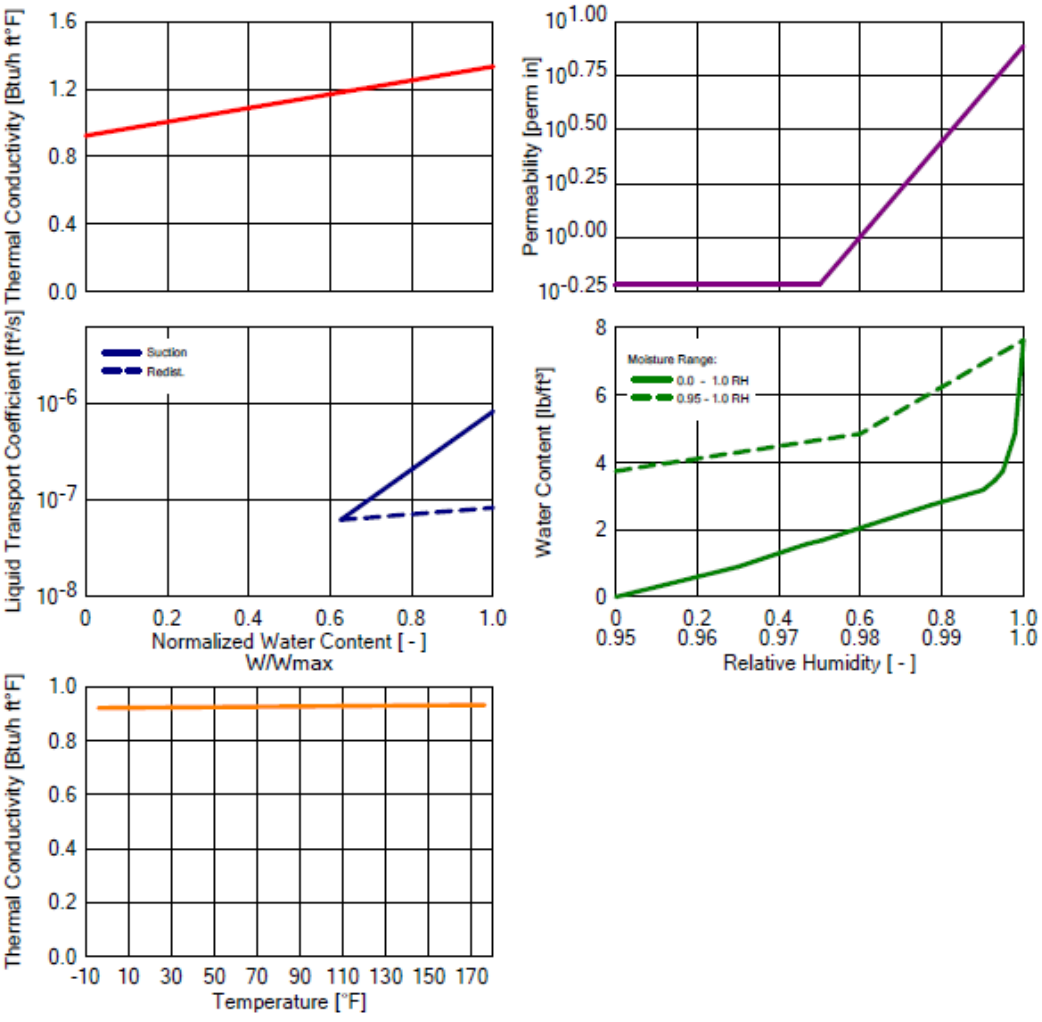

WUFI Pro 6.3

Material: *XPS 1.5inch

Property	Unit	Value
Bulk density	[lb/ft³]	1.604
Porosity	[ft³/ft³]	0.02
Specific Heat Capacity, Dry	[Btu/lb°F]	0.351
Thermal Conductivity, Dry, 50°F	[Btu/h ft°F]	0.017
Permeability	[perm in]	1.2
Reference Water Content	[lb/ft³]	0.015
Free Water Saturation	[lb/ft³]	0.999
Water Absorption Coefficient	[lb/in²s^0.5]	0.0000010
Temp-dep. Thermal Cond. Supplement	[Btu/h ft°F²]	0.0000420

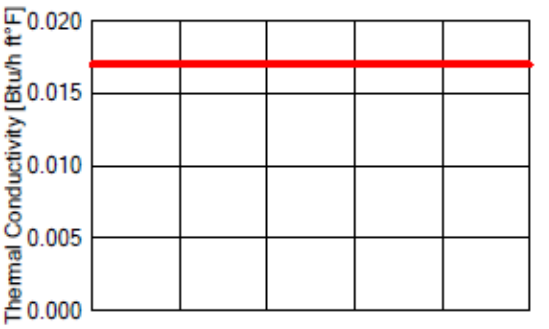

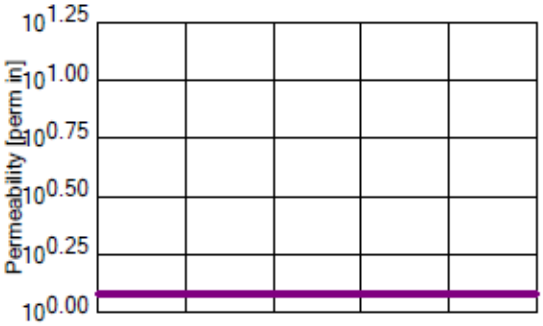

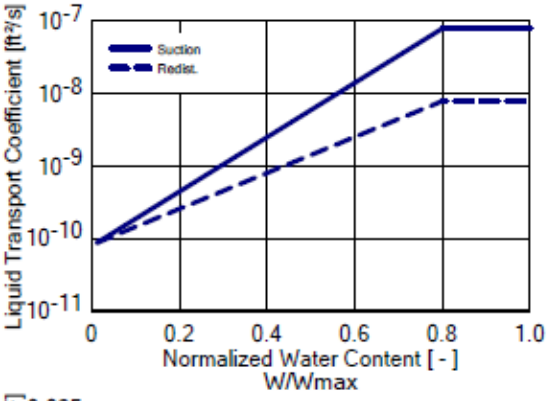

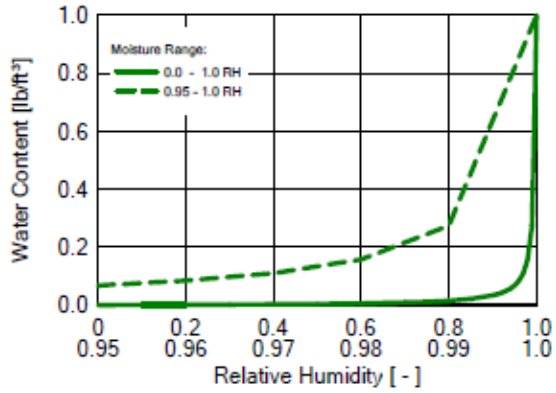

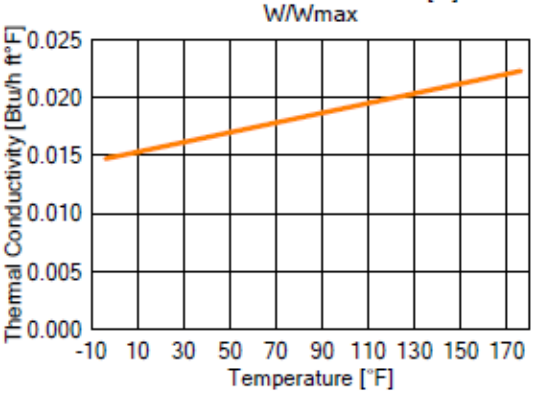

WUFI Pro 6.3

Material: *Oriented Strand Board - new

Property	Unit	Value
Bulk density	[lb/ft³]	40.5782
Porosity	[ft³/ft³]	0.95
Specific Heat Capacity, Dry	[Btu/lb°F]	0.449
Thermal Conductivity, Dry, 50°F	[Btu/h ft°F]	0.0532
Permeability	[perm in]	0.1585
Reference Water Content	[lb/ft³]	5.2003
Free Water Saturation	[lb/ft³]	29.3411
Water Absorption Coefficient	[lb/in²s^0.5]	0.0000031
Temp-dep. Thermal Cond. Supplement	[Btu/h ft°F²]	0.0000642